

A Study of the Coupled Gravitational and Electromagnetic Perturbations to the Reissner–Nordstrom Black Hole: The Scattering Matrix, Energy Conversion, and Quasi-Normal Modes

D. L. Gunter

Phil. Trans. R. Soc. Lond. A 1980 **296**, 497–526
doi: 10.1098/rsta.1980.0190

Email alerting service

Receive free email alerts when new articles cite this article - sign up in the box at the top right-hand corner of the article or click [here](#)

To subscribe to *Phil. Trans. R. Soc. Lond. A* go to: <http://rsta.royalsocietypublishing.org/subscriptions>

A STUDY OF THE COUPLED GRAVITATIONAL AND
 ELECTROMAGNETIC PERTURBATIONS TO THE
 REISSNER-NORDSTRÖM BLACK HOLE: THE
 SCATTERING MATRIX, ENERGY CONVERSION, AND
 QUASI-NORMAL MODES

By D. L. GUNTER

Department of Physics, University of Chicago, Chicago, Illinois 60637 U.S.A.

(Communicated by S. Chandrasekhar, F.R.S. – Received 30 October 1978
 – Revised 4 May 1979)

CONTENTS

	PAGE
1. INTRODUCTION	498
2. THE EQUATIONS OF THE PROBLEM	498
3. THE SCATTERING MATRIX	500
4. THE ELECTROMAGNETIC-GRAVITATIONAL CONVERSION COEFFICIENTS	502
5. THE QUASI-NORMAL MODES	502
6. CONCLUSION	505
REFERENCES	506

The reflection and absorption, by the charged spherically symmetric Reissner-Nordström black hole, of an arbitrary superposition of gravitational and electromagnetic waves, with time dependence $e^{i\sigma t}$ and analyzed into spherical harmonics of various orders l , are expressed in terms of the complex reflection and transmission amplitudes (for incident waves) by two one-dimensional potential barriers. These amplitudes, expressed in terms of eight quantities (and composing the scattering matrix), are tabulated for various values of σ , l ($= 2, 3$, and 6) and charge of the black hole.

By virtue of the coupling of electromagnetic and gravitational perturbations by the charge of the black hole, the energy in an incident wave, which is purely gravitational, is, in part, reflected as electromagnetic waves; and conversely. This transformation of incident gravitational energy into electromagnetic energy (and vice versa) is expressed in terms of a conversion factor C and plotted in a series of graphs as a function of σ for various values of l and the charge on the black hole Q_* .

Finally, the complex frequencies belonging to the quasi-normal modes (i.e., solutions of the underlying wave equations which correspond to purely outgoing waves at infinity and purely ingoing waves at the horizon) are tabulated. It is found that the imaginary part of these frequencies (which determine the damping of arbitrary initial perturbations of the black hole) is very nearly the same for all modes (with different l 's) and Q_* .

1. INTRODUCTION

The Reissner–Nordström metric represents a spherical symmetric static space-time appropriate for a black hole with charge (Q_*) and mass (M), and is a solution of the coupled Einstein–Maxwell equations. The coupling of electromagnetic and gravitational perturbations, by virtue of the charge on the black hole, results in the transformation of a fraction of an incident flux of pure gravitational energy into electromagnetic energy; and conversely. More generally, the manner in which an arbitrary superposition of electromagnetic and gravitational waves will be reflected and absorbed by the black hole can be expressed in terms of a set of complex amplitudes comprising a ‘scattering matrix’. These aspects of the theory of the perturbations of the Reissner–Nordström black hole will be examined in this paper. In contrast to current discussions of this problem (cf. Matzner 1976), we shall not limit ourselves to the zero-frequency limit; also, we shall distinguish the parity of the incident waves.

Besides tabulating the various quantities which determine the scattering matrix, we shall consider the quasi-normal modes (cf. Chandrasekhar & Detweiler 1975) of the Reissner–Nordström black hole. The quasi-normal modes describe the asymptotic behaviour of how the black hole, initially disturbed in some arbitrary way, will approach equilibrium (cf. Cunningham *et al.* 1978); they describe the ‘ringing’ of the black hole.

2. THE EQUATIONS OF THE PROBLEM

From a consideration of the metric perturbations (with a time dependence $e^{i\omega t}$ and analysed into spherical harmonics of various orders l), Moncrief (1974*a, b*; 1975) has derived two pairs of one-dimensional wave equations appropriate for odd, respectively, even parity. Moncrief’s equations, in the form Chandrasekhar (1979) has recently written, are summarized in

$$\left[\frac{d^2}{dr_*^2} - \sigma^2 - V_i^{(\pm)} \right] Z_i^{(\pm)} = 0, \quad (1)$$

where

$$V_i^{(-)} = (\Delta/r^5) [(\mu^2 + 2) r - q_j(1 + q_i/\mu^2 r)], \quad (2)$$

$$V_i^{(+)} = V_i^{(-)} + 2q_j \frac{d}{dr_*} \left[\frac{\Delta}{r^3(\mu^2 r + q_j)} \right], \quad (3)$$

$$\Delta = r^2 - 2Mr + Q_*^2, \quad \mu^2 = (l-1)(l+2), \quad (4)$$

$$q_1 = 3M + \sqrt{(9M^2 + 4Q_*^2\mu^2)}, \quad q_2 = 3M - \sqrt{(9M^2 + 4Q_*^2\mu^2)}, \quad (5)$$

and

$$i, j = 1, 2 \quad (i \neq j). \quad (6)$$

The variable r_* is related to r by the equation

$$\frac{dr_*}{dr} = \frac{r^2}{\Delta}, \quad (7)$$

and the superscripts (\pm) distinguish the even $(+)$ and the odd $(-)$ parity.

PERTURBATIONS OF REISSNER-NORDSTRÖM BLACK HOLE 499

Chandrasekhar has shown (1979, equation (67)) that a solution $Z_i^{(-)}$, appropriate for odd parity, can be deduced from a solution $Z_i^{(+)}$, appropriate for even parity, from the relation

$$[\mu^2(\mu^2+2) - 2i\sigma q_j] Z_i^{(-)} = \left[\mu^2(\mu^2+2) + \frac{2q_j^2 A}{r^3(\mu^2 r + q_j)} \right] Z_i^{(+)} - 2q_j \frac{d}{dr_*} Z_i^{(+)}. \quad (8)$$

This relation greatly simplifies the analysis of the Reissner-Nordström perturbations: for once a solution appropriate for one parity has been obtained, the solution for the opposite parity follows immediately.

In the present paper the equation for odd parity is integrated for the various problems; the corresponding results for even parity were deduced by transforming the solutions for odd parity in accordance with equation (8).

Since the potentials $V_i^{(\pm)}$ which appear in the one-dimensional wave equations are of short range, we can seek solutions of the equations which have the asymptotic behaviour,

$$\left. \begin{aligned} Z_i^{(\pm)} &\rightarrow e^{i\sigma r_*} + R_i^{\frac{1}{2}} \exp(i\delta_i^{r,\pm} - i\sigma r_*) & (r_* \rightarrow \infty), \\ &\rightarrow T_i^{\frac{1}{2}} \exp(i\delta_i^t + i\sigma r_*) & (r_* \rightarrow -\infty), \end{aligned} \right\} \quad (9)$$

where the reflection and transmission coefficients R_i and T_i as well as the phases δ_i^t are the same for both parities as Chandrasekhar has shown (Chandrasekhar 1979, equations (69) and (70)). Also,

$$\delta_i^{r,+} - \delta_i^{r,-} = \arg \left[\frac{\mu^2(\mu^2+2) - 2i\sigma q_j}{\mu^2(\mu^2+2) + 2i\sigma q_j} \right] \quad (i, j = 1, 2; i \neq j). \quad (10)$$

Since the potentials $V_i^{(\pm)}$ are real, we have the conservation laws

$$R_i + T_i = 1. \quad (11)$$

From equation (9) it follows that the scattering process is uniquely specified by the amplitudes of the reflected and transmitted waves. And these amplitudes are determined by the eight quantities

$$R_1, R_2, \delta_1^{r,\pm}, \delta_2^{r,\pm}, \delta_1^t \text{ and } \delta_2^t.$$

In order to determine how an incident superposition of electromagnetic and gravitational waves will be reflected and absorbed by the black hole, we must relate the amplitudes of the incident waves to the amplitudes of $Z_i^{(\pm)}$. If $H_i^{(\pm)}$ and $H_2^{(\pm)}$ represent the amplitudes of the electromagnetic and the gravitational waves, respectively, then the required relations are

$$\left. \begin{aligned} H_1^{(\pm)} &= Z_1^{(\pm)} \cos \psi - Z_2^{(\pm)} \sin \psi, \\ H_2^{(\pm)} &= Z_2^{(\pm)} \cos \psi + Z_1^{(\pm)} \sin \psi, \\ Z_1^{(\pm)} &= H_1^{(\pm)} \cos \psi + H_2^{(\pm)} \sin \psi, \\ Z_2^{(\pm)} &= H_2^{(\pm)} \cos \psi - H_1^{(\pm)} \sin \psi, \end{aligned} \right\} \quad (12)$$

where

$$\sin 2\psi = \mp 2\sqrt{-q_1 q_2 / (q_1 - q_2)^2}.$$

Consequently, for solutions $Z_i^{(\pm)}$ which correspond to incident and reflected waves given by

$$Z_{i,\text{inc}}^{(\pm)} = A_i^{(\pm)} e^{i\sigma r_*} \quad \text{and} \quad Z_{i,\text{ref}}^{(\pm)} = A_i^{(\pm)} R_i^{\frac{1}{2}} \exp(i\delta_i^{r,\pm} - i\sigma r_*),$$

the reflected fluxes of electromagnetic and gravitational energies are proportional to

$$|H_1^{(\pm)}|^2 = A_1^{(\pm)2} \mathbb{R}_1 \cos^2 \psi + A_2^{(\pm)2} \mathbb{R}_2 \sin^2 \psi - 2A_1^{(\pm)} A_2^{(\pm)} \mathbb{R}_1^{\frac{1}{2}} \mathbb{R}_2^{\frac{1}{2}} \cos \Delta_{12}^{r,\pm} \sin \psi \cos \psi \quad (13)$$

and

$$|H_2^{(\pm)}|^2 = A_1^{(\pm)2} \mathbb{R}_1 \sin^2 \psi + A_2^{(\pm)2} \mathbb{R}_2 \cos^2 \psi + 2A_1^{(\pm)} A_2^{(\pm)} \mathbb{R}_1^{\frac{1}{2}} \mathbb{R}_2^{\frac{1}{2}} \cos \Delta_{12}^{r,\pm} \sin \psi \cos \psi, \quad (14)$$

where

$$\Delta_{12}^{r,\pm} = \delta_1^{r,\pm} - \delta_2^{r,\pm}. \quad (15)$$

When the incident wave is a purely electromagnetic wave,

$$A_1^{(\pm)} = \cos \psi \quad \text{and} \quad A_2^{(\pm)} = -\sin \psi$$

and equations (13) and (14) give

$$|H_1^{(\pm)}|^2 = \mathbb{R}_1 \cos^4 \psi + \mathbb{R}_2 \sin^4 \psi + 2\mathbb{R}_1^{\frac{1}{2}} \mathbb{R}_2^{\frac{1}{2}} \cos \Delta_{12}^{r,\pm} \sin^2 \psi \cos^2 \psi \quad (16)$$

and

$$|H_2^{(\pm)}|^2 = (\mathbb{R}_1 + \mathbb{R}_2 - 2\mathbb{R}_1^{\frac{1}{2}} \mathbb{R}_2^{\frac{1}{2}} \cos \Delta_{12}^{r,\pm}) \sin^2 \psi \cos^2 \psi. \quad (17)$$

Similarly, when the incident wave is purely gravitational,

$$A_1^{(\pm)} = \sin \psi \quad \text{and} \quad A_2^{(\pm)} = \cos \psi$$

and equations (13) and (14) give

$$|H_1^{(\pm)}|^2 = (\mathbb{R}_1 + \mathbb{R}_2 - 2\mathbb{R}_1^{\frac{1}{2}} \mathbb{R}_2^{\frac{1}{2}} \cos \Delta_{12}^{r,\pm}) \sin^2 \psi \cos^2 \psi \quad (18)$$

and

$$|H_2^{(\pm)}|^2 = \mathbb{R}_1 \sin^4 \psi + \mathbb{R}_2 \cos^4 \psi + 2\mathbb{R}_1^{\frac{1}{2}} \mathbb{R}_2^{\frac{1}{2}} \cos \Delta_{12}^{r,\pm} \sin^2 \psi \cos^2 \psi. \quad (19)$$

From a comparison of the foregoing equations, it follows that the fraction of incident energy C^\pm which is entirely of one form (electromagnetic or gravitational) that is converted into reflected energy of the other form is the same whichever form we consider. This conversion factor is given by

$$C^\pm = (\mathbb{R}_1 + \mathbb{R}_2 - 2\mathbb{R}_1^{\frac{1}{2}} \mathbb{R}_2^{\frac{1}{2}} \cos \Delta_{12}^{r,\pm}) \sin^2 \psi \cos^2 \psi. \quad (20)$$

It should be emphasized that C^\pm depends on parity – one of the few instances in black-hole physics in which parity is relevant. (It should be pointed out in this connection that there is no such dependence on parity when we consider the transmitted fluxes since the phases of the transmitted amplitudes do not depend on parity.)

3. THE SCATTERING MATRIX

We have seen that the scattering process is entirely described by the complex amplitudes

$$\mathbb{R}_i^{\frac{1}{2}} e^{i\delta_i^{r,\pm}} \quad \text{and} \quad \mathbb{T}_i^{\frac{1}{2}} e^{i\delta_i^t}$$

of the reflected and transmitted waves; and as we have indicated it will suffice to integrate the one-dimensional wave equation, for the odd or the even parity, with the boundary conditions specified in equation (9). Also, as we have stated, it is convenient to use the equations for the odd parity (since they are simpler).

Since the boundary conditions are imposed for $r_* \rightarrow \pm \infty$, it is necessary that we obtain asymptotic series expansions for the solution valid at $\pm \infty$, so that the numerical integration

PERTURBATIONS OF REISSNER–NORDSTRÖM BLACK HOLE 501

of the equations can be started (and ended) at finite r_* . We obtain the requisite asymptotic expansions in the following manner.

Far from the black hole, we assume an expansion of the form

$$Z_i^{(-)} = e^{ie\sigma r_*} \sum_{n=1}^{\infty} A_n^{(i)} r^{1-n} \quad (r_* \rightarrow +\infty) \quad (21)$$

where $\epsilon = +1$ for ingoing waves and $\epsilon = -1$ for outgoing waves. Substituting this expansion in the wave equation for $Z_i^{(-)}$, we obtain the recurrence relation

$$\begin{aligned} 2i\sigma\epsilon(n-1) A_n^{(i)} &= [(n-1)(n-2) - (\mu^2 + 2)] A_{n-1}^{(i)} \\ &+ [q_j - 2M(n-1)(n-3)] A_{n-2}^{(i)} \quad (i, j = 1, 2; i \neq j) \\ &+ [n(n-5) Q_*^2] A_{n-3}^{(i)} \quad \text{and} \quad (n \geq 0), \end{aligned} \quad (22)$$

together with $A_1^{(i)} = 1$, required by the boundary condition for $r_* \rightarrow +\infty$.

For $r_* \rightarrow -\infty$ and $r \rightarrow r_+ + 0$, where $r_{\pm} = M \pm \sqrt{(M^2 - Q_*^2)}$, we assume an expansion of the form

$$Z_i^{(-)} = e^{i\sigma r_*} \sum_{n=1}^{\infty} B_n^{(i)} (r - r_+)^{n-1} \quad (23)$$

and obtain the following recurrence relation:

$$\begin{aligned} [2i\sigma r_+^4 + 2Mr_+^2 - 2Q_*^2 r_+ + (n-1)(r_+ - r_-) r_+^2] n B_{n+1}^{(i)} \\ = [(\mu^2 + 2)r_+^2 - q_j r_+ + 4Q_*^2 - (n-1)(n-2)(3r_+ - 2r_-)r_+ - (n-1)(8i\sigma r_+^3 + 4Mr_+ - 2Q_*^2)] B_n^{(i)} \\ + [2(\mu^2 + 2)r_+ - q_j - (n-2)(n-3)(3r_+ - r_-) - (n-2)(12i\sigma r_+^2 + 2M)] B_{n-1}^{(i)} \\ + [(\mu^2 + 2) - (n-3)(n-4 + 8i\sigma r_+)] B_{n-2}^{(i)} + [(4-n)(2i\sigma)] B_{n-3}^{(i)} \quad (n \geq 0), \end{aligned} \quad (24)$$

together with $B_1^{(i)} = 1$.

The foregoing asymptotic expansions allow the integrations to be started at $r_* = -20$ and ended at $r_* = 55$. The integrations were started at $r_* = -20$ and integrated outward to r_* sufficiently large that with the aid of the asymptotic expansion (21) the wave could be decomposed into an outgoing and an ingoing wave.

Description of the tables

The results of the integrations are summarized in tables 1a–4c. In each table, the values of

$$\mathbb{R}_1, \mathbb{R}_2, \delta_2^t, \delta_2^{r,\pm}, \Delta_{12}^t = \delta_1^t - \delta_2^t \quad \text{and} \quad \Delta_{12}^{r,\pm} = \delta_1^{r,\pm} - \delta_2^{r,\pm}$$

are listed for a particular value of l and Q_* and for values of $M\sigma$ for which the reflection coefficients are significant.

In particular, tables 1a–1c refer to the Reissner–Nordström black hole for $l = 2, 3$, and 6; and tables 4a–4c refer to $Q_* = 0.99M$.

An examination of the numerical results summarized in these tables reveals the following features:

(1) $\mathbb{R}_i \rightarrow 1$ as $\sigma \rightarrow 0$. It remains close to unity for σ less than a certain critical frequency ($\sim 0.2l/M$) beyond which it decreases to zero exponentially like $\exp(-15.2M\sigma)$. The critical frequency for \mathbb{R}_1 is always greater than that for \mathbb{R}_2 .

(2) The phase angles show few obvious patterns. However, $\Delta_{12}^{r,+}$ and $\Delta_{12}^{r,-}$ tend to zero for $\sigma \rightarrow 0$. For $l \geq 2$, Δ_{12}^t tends to zero for $\sigma \rightarrow 0$. And for $l = 1$, $\Delta_{12}^t \rightarrow \frac{1}{2}\pi$ as $\sigma \rightarrow 0$.

4. THE ELECTROMAGNETIC-GRAVITATIONAL CONVERSION COEFFICIENTS

The conversion coefficient C^\pm as defined in § 2 is

$$C^\pm = (\mathbb{R}_1 + \mathbb{R}_2 - 2\mathbb{R}_1^{\frac{1}{2}}\mathbb{R}_2^{\frac{1}{2}} \cos \Delta_{12}^{r_1^\pm}) \sin^2 \psi \cos^2 \psi,$$

where

$$\sin 2\psi = \mp 2\sqrt{(-q_1 q_2)/(q_1 - q_2)^2}.$$

For $l = 1$, $\sin \psi = 0$ and $C^\pm = 0$. For $l \geq 2$, the conversion factors are significant in a narrow band of frequencies. For $\sigma \rightarrow \infty$, $\mathbb{R}_i \rightarrow 0$ and all the incident radiation is absorbed. For $\sigma \rightarrow 0$, while $\mathbb{R}_i \rightarrow 1$, the phase differences $\Delta_{12}^{r_1^\pm} \rightarrow 0$; this latter fact has the consequence that C^\pm also tends to zero in this limit.

The dependence of C^\pm on σ and on l is illustrated in figures 1–10, for various values of Q_* . As one might have expected, C^\pm increases with Q_* .

We may notice the following aspects of the dependence of C^\pm on σ . For $\sigma \rightarrow 0$, C^\pm is largely determined by $\Delta_{12}^{r_1^\pm}$, while the exponentially decreasing \mathbb{R}_i for $\sigma > 0.2l/M$ manifests itself in C^\pm having a maximum value at about this critical frequency and decreasing beyond this frequency. (The hump which appears in the curve for $Q_* = 0.99M$ is a result of \mathbb{R}_1 and \mathbb{R}_2 decreasing exponentially beyond slightly different critical frequencies; but this effect is not exhibited until Q_* becomes very close to M .)

A major feature of C^\pm is its dependence on parity. We observe that even parity waves are characterized by larger conversion factors than the odd parity waves. The difference becomes more pronounced for increasing Q_* ; but becomes less pronounced for increasing l .

It will also be observed that the band of frequencies in which C^\pm is appreciable becomes wider for increasing values of l . Two factors contribute to this effect. First, the potential barriers around the black hole become increasingly difficult to penetrate for increasing values of l ; and in consequence, the frequencies for which \mathbb{R}_i become appreciable also increase. And second the factor $\sin^2 \psi \cos^2 \psi$ in C^\pm also increases with l .

5. THE QUASI-NORMAL MODES

The quasi-normal modes of the Reissner–Nordström black hole were determined by the same technique described by Chandrasekhar & Detweiler (1975). The boundary conditions for quasi-normal modes are that the radiation is purely outgoing at infinity and purely ingoing on the horizon. These boundary conditions can be satisfied only for characteristic frequencies which are complex. Therefore, the solutions for $Z_i^{(\pm)}$ grow exponentially as $r_* \rightarrow \pm \infty$. This asymptotic behaviour makes numerical integration of the wave equation (1) for $Z_i^{(\pm)}$ very difficult. However, the transformation

$$Z_j = \exp(i \int \phi_j dr_*) \quad (25)$$

or

$$\phi_j = -\frac{i}{Z_j} \frac{d}{dr_*} Z_j$$

leads to equations of the Riccati type and the difficulty associated with the exponential growth can be avoided. Note that we are not distinguishing parity, since Chandrasekhar's relation

between the even and the odd parity solutions guarantees that $Z_i^{(+)}$ and $Z_i^{(-)}$ have quasi-normal modes which are related and with the same characteristic frequencies.

The equation satisfied by ϕ_j is

$$i\phi_j \frac{d}{dr_*} + \sigma^2 - \phi_j^2 - V_j^{(-)} = 0, \quad (26)$$

where we have chosen $V_j^{(-)}$ since it is simpler than $V_j^{(+)}$. The boundary conditions for ϕ_j appropriate for quasi-normal modes are

$$\phi_j \rightarrow -\sigma \quad \text{as} \quad r_* \rightarrow \infty, \quad (27)$$

and

$$\phi_j \rightarrow \sigma \quad \text{as} \quad r_* \rightarrow -\infty. \quad (28)$$

To satisfy these conditions we must consider σ as a characteristic value parameter.

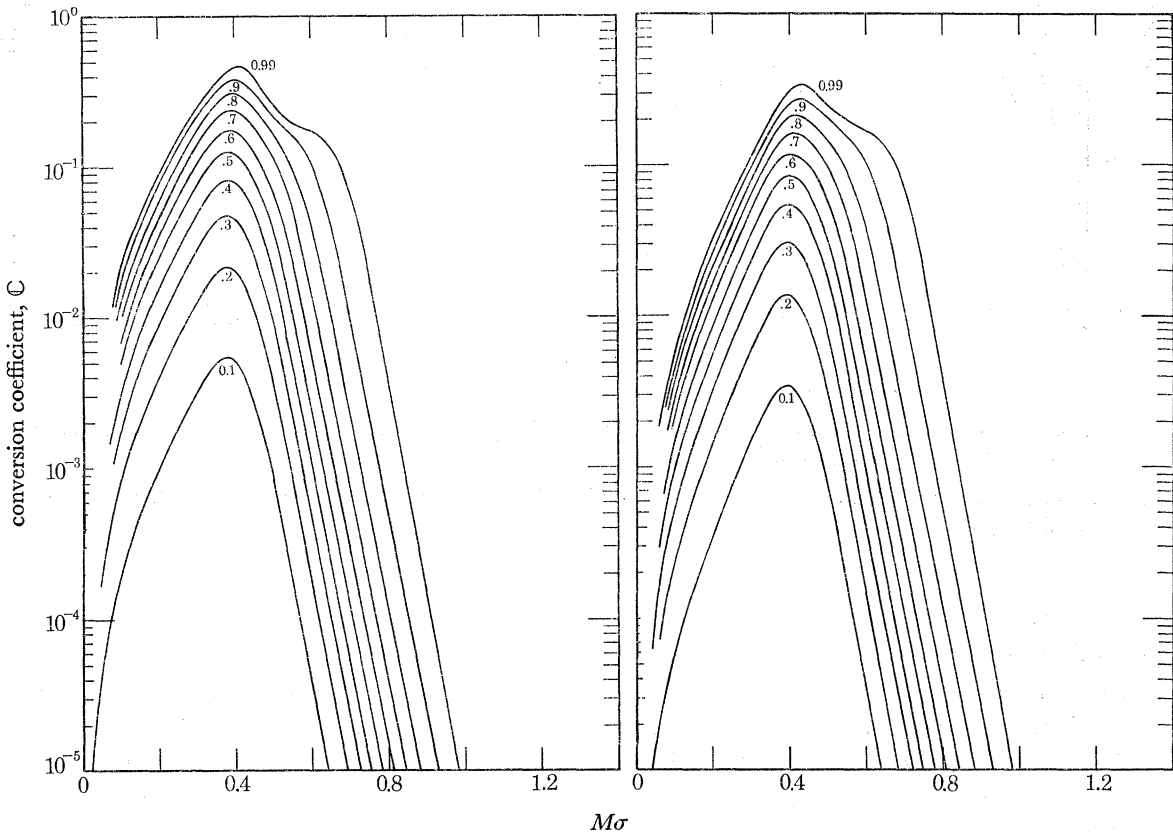


FIGURE 1

M σ

FIGURE 2

FIGURE 1. The conversion coefficient C^+ for the even-parity perturbations belonging to $l = 2$. Each curve is labelled by the charge Q_* (ranging from $Q_* = 0.1M$ to $Q_* = 0.99M$). It will be observed that the conversion coefficients become significant in the frequency-range $0.2 \leq M\sigma \leq 0.7$; and C^+ attains its maximum at $M\sigma \approx 0.4$ for all values of Q_* . The low-frequency behaviour ($M\sigma < 0.4$) is determined by $A_{12}^{l=2+}$; while the high-frequency behaviour ($M\sigma > 0.6$) is determined by the exponential decrease of the reflection coefficients beyond $M\sigma \approx 0.4$.

FIGURE 2. The conversion coefficient C^- for the odd-parity perturbations belonging to $l = 2$. Each curve is labelled by the charge Q_* (ranging from $Q_* = 0.1M$ to $Q_* = 0.99M$). Notice that conversion coefficients for even-parity (in figure 1) are larger than those for odd-parity in this figure.

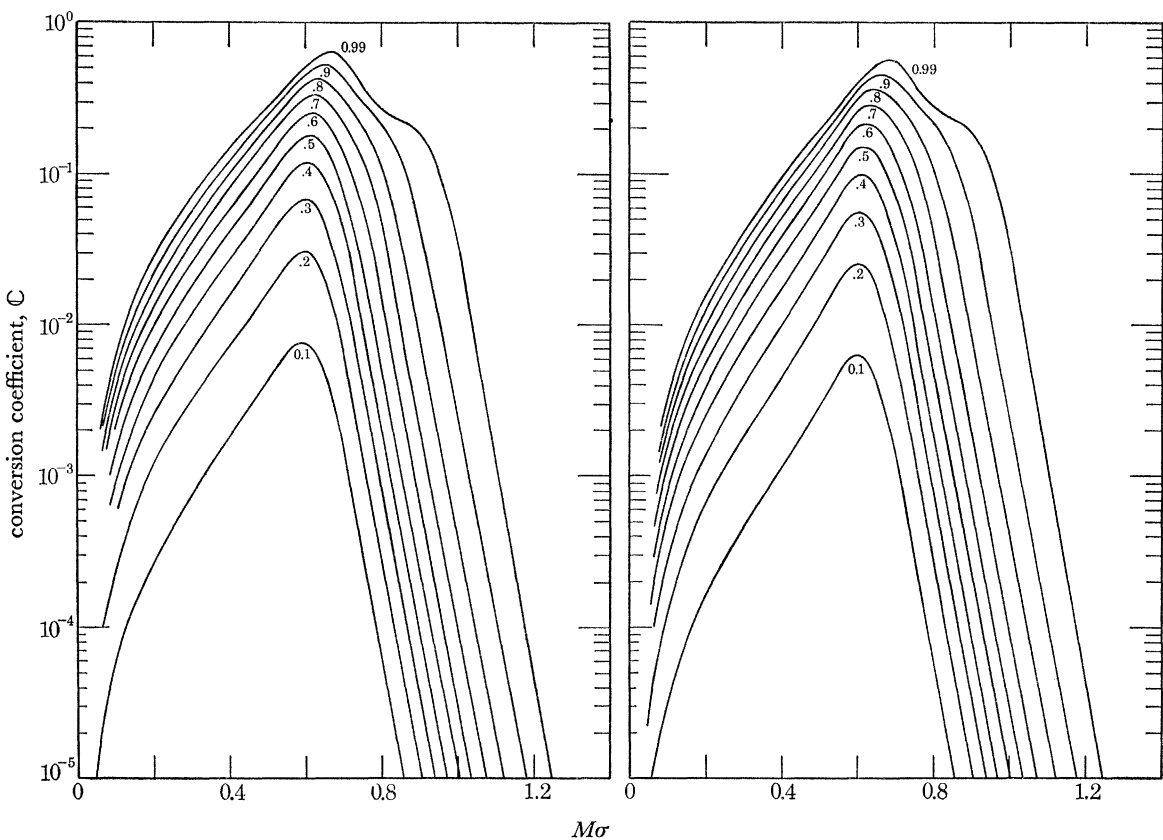


FIGURE 3

FIGURE 4

FIGURE 3. The conversion coefficient C^+ for the even-parity perturbations belonging to $l = 3$. Each curve is labelled by the charge Q_* to which it belongs.

FIGURE 4. The conversion coefficient C^- for the odd-parity perturbations belonging to $l = 3$. Each curve is labelled by the charge Q_* to which it belongs.

The search for quasi-normal modes involves guessing the frequency σ and then integrating equation (26) to check whether both boundary conditions are satisfied. For each frequency two integrations are performed. First, ϕ_j is integrated inward from $r_* = 25$ with the use of boundary condition (27) to start the integration. Then ϕ_j is integrated outward from $r_* = -18$ using the boundary condition (28). Finally, the two integrations are compared at the point where ϕ_j varies most rapidly. The requirement that the two integrations agree at the common point determines the characteristic frequency. In this way the complex-frequency plane can be searched for quasi-normal modes.

Just as for the calculation of the scattering matrix, the boundary conditions at finite distances must be evaluated using asymptotic expansions. The same recursion relations may be used to determine the asymptotic expansions as were used in § 3, except that the frequency is complex and ϕ_j must be evaluated using equation (25). Care must be taken not to exceed the accuracy of the asymptotic expansion by trying to use too many terms.

Tables 5 and 6 list the quasi-normal modes which are nearest to the real axis in the complex-frequency plane. The quasi-normal modes for Z_1 are listed in table 5 for various values of l and for various charges Q_* . And in table 6 we list the quasi-normal modes of Z_2 . In both of

PERTURBATIONS OF REISSNER-NORDSTRÖM BLACK HOLE 505

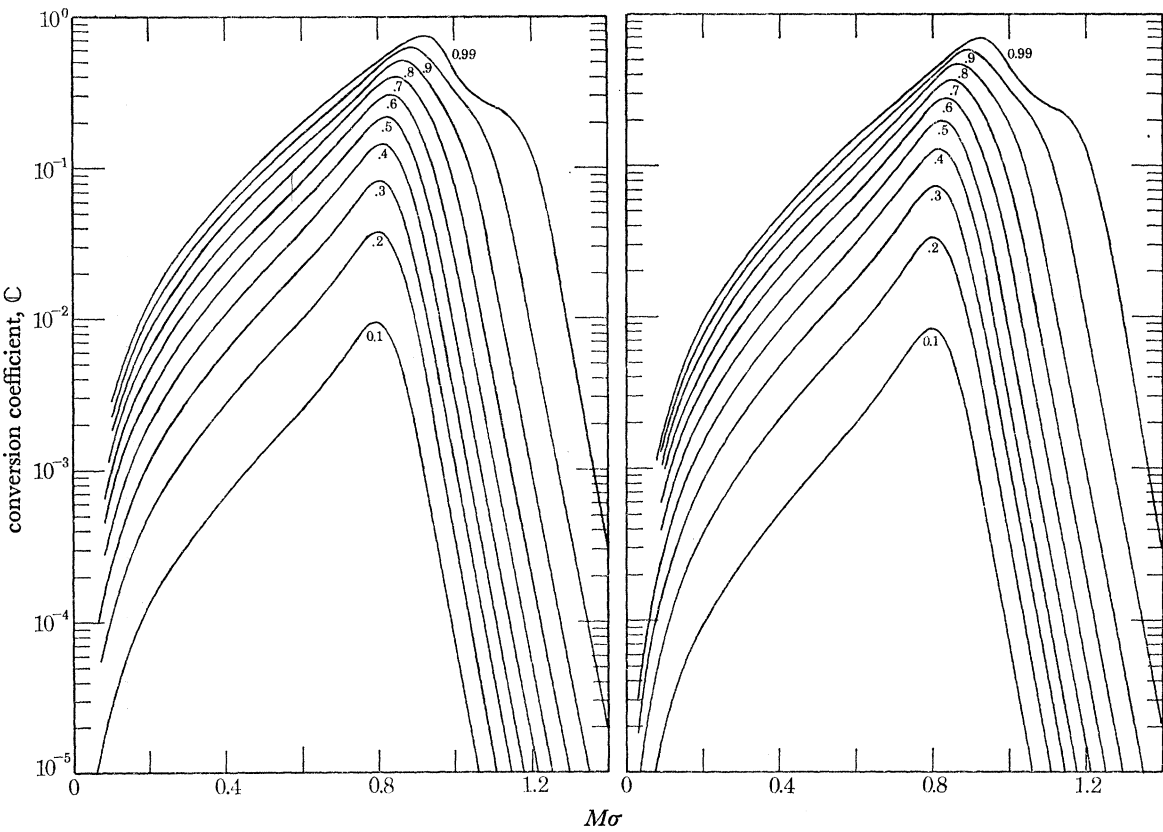


FIGURE 5

FIGURE 6

FIGURE 5. The conversion coefficient C^+ for the even-parity perturbations belonging to $l = 4$. Each curve is labelled by the charge Q_* to which it belongs.

FIGURE 6. The conversion coefficient C^- for the odd-parity perturbations belonging to $l = 4$. Each curve is labelled by the charge Q_* to which it belongs.

these tables the complex frequencies have essentially a constant imaginary part, $\text{Im}(M\sigma) \simeq 0.09$. The reason why all these modes have the same imaginary part is not clear.

A second set of quasi-normal modes with larger imaginary parts has also been determined. This second set of modes has nearly the same $\text{Re}(\sigma)$; but $\text{Im}(\sigma) \simeq 0.3/M$. This set of quasi-normal modes is physically less significant since they decay more rapidly. It should be noted that the reliability of the numerical analysis diminishes for frequencies with large imaginary parts. For these reasons only the quasi-normal modes nearest the real axis have been tabulated.

6. CONCLUSIONS

While the scattering matrix and the complex characteristic frequencies of the quasi-normal modes have been determined for perturbations of the Reissner-Nordström black hole, there are numerous interesting questions that are left unresolved by this numerical treatment. In particular, the origin of the uniform exponential decrease of R_i for σ greater than a certain critical σ (depending on l) is not clear. Similarly, one should like to understand why $\Delta_{12}^{r,+}$ and $\Delta_{12}^{r,-} \rightarrow 0$ for $\sigma \rightarrow 0$. And in the context of the quasi-normal modes we may ask why the imaginary part of the characteristic frequency is (as far as the numerical integrations show) so nearly independent of the various parameters of the problem.

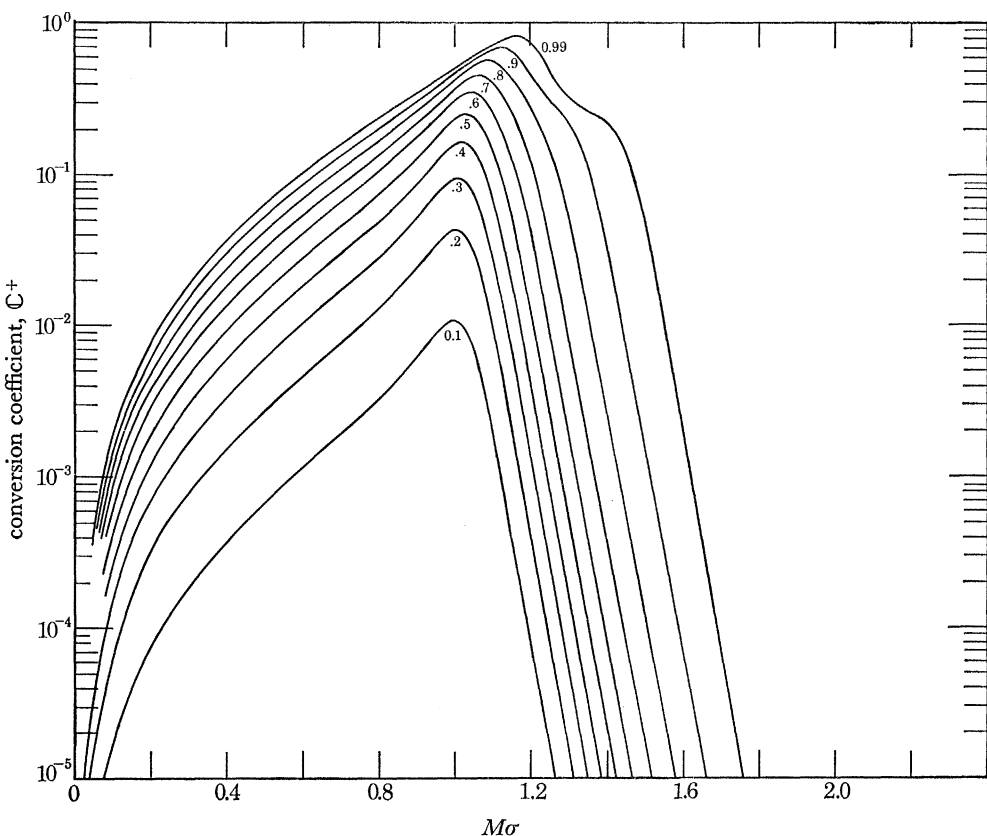


FIGURE 7. The conversion coefficient C^+ for the even-parity perturbations belonging to $l = 5$. Each curve is labelled by the charge Q_* to which it belongs.

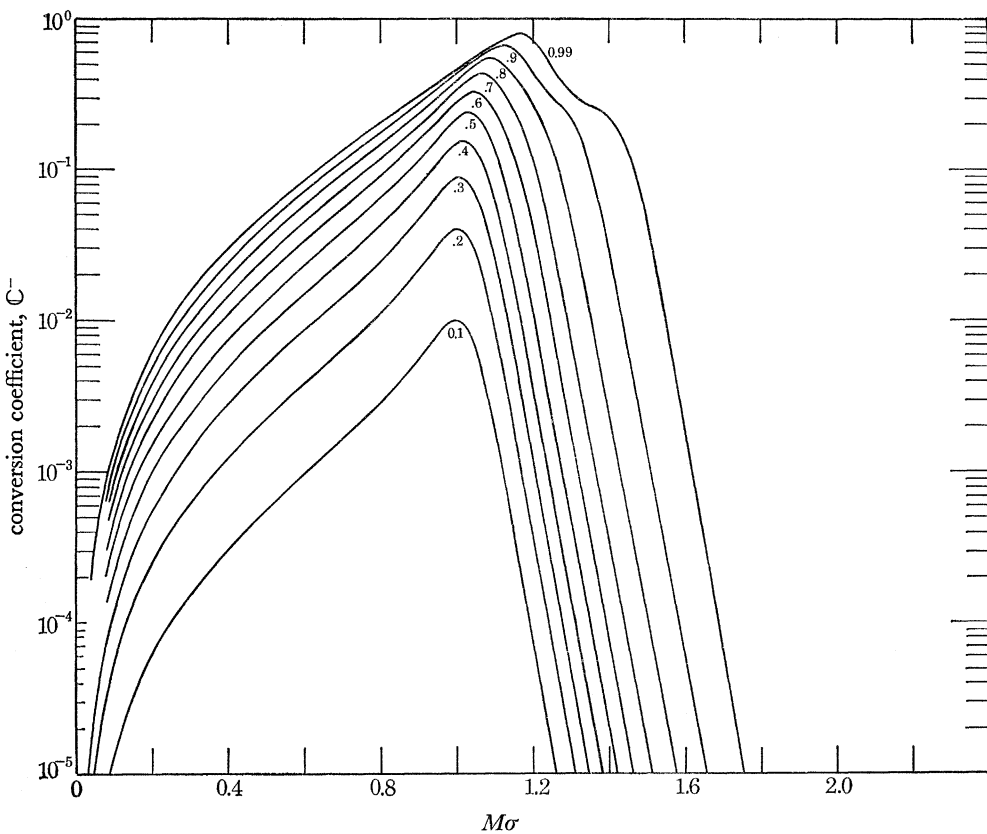


FIGURE 8. The conversion coefficient C^- for the odd-parity perturbations belonging to $l = 5$. Each curve is labelled by the charge Q_* to which it belongs.

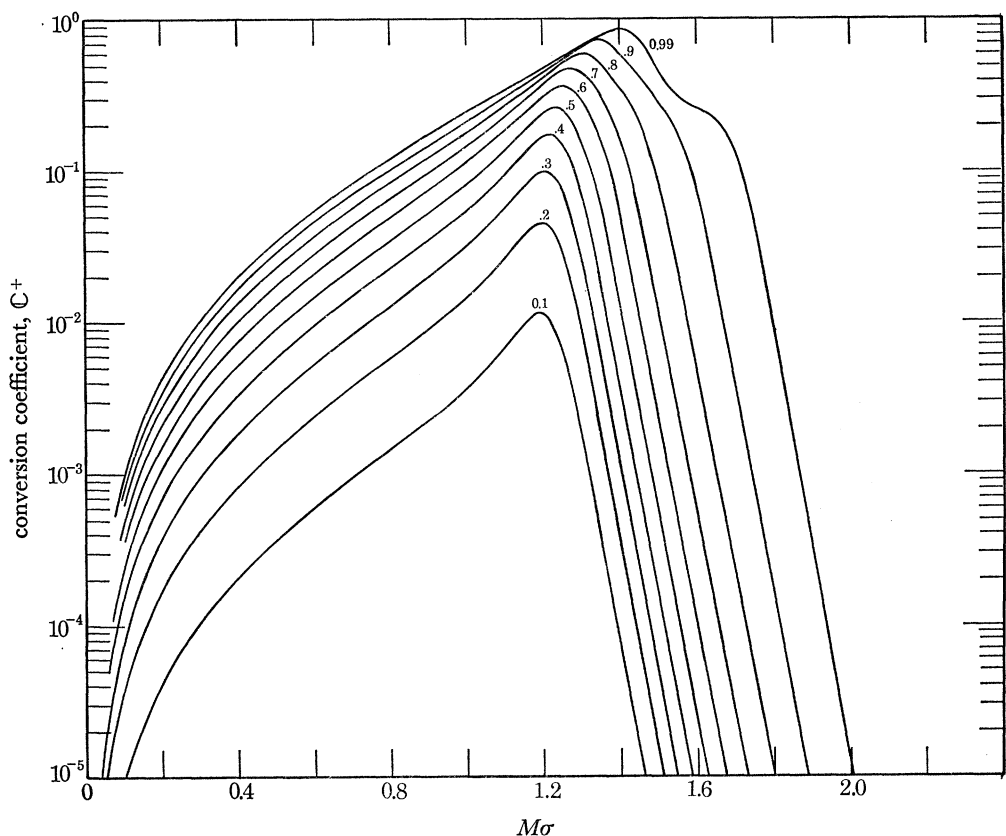


FIGURE 9. The conversion coefficient C^+ for the even-parity perturbations belonging to $l = 6$.
Each curve is labelled by the charge Q_* to which it belongs.

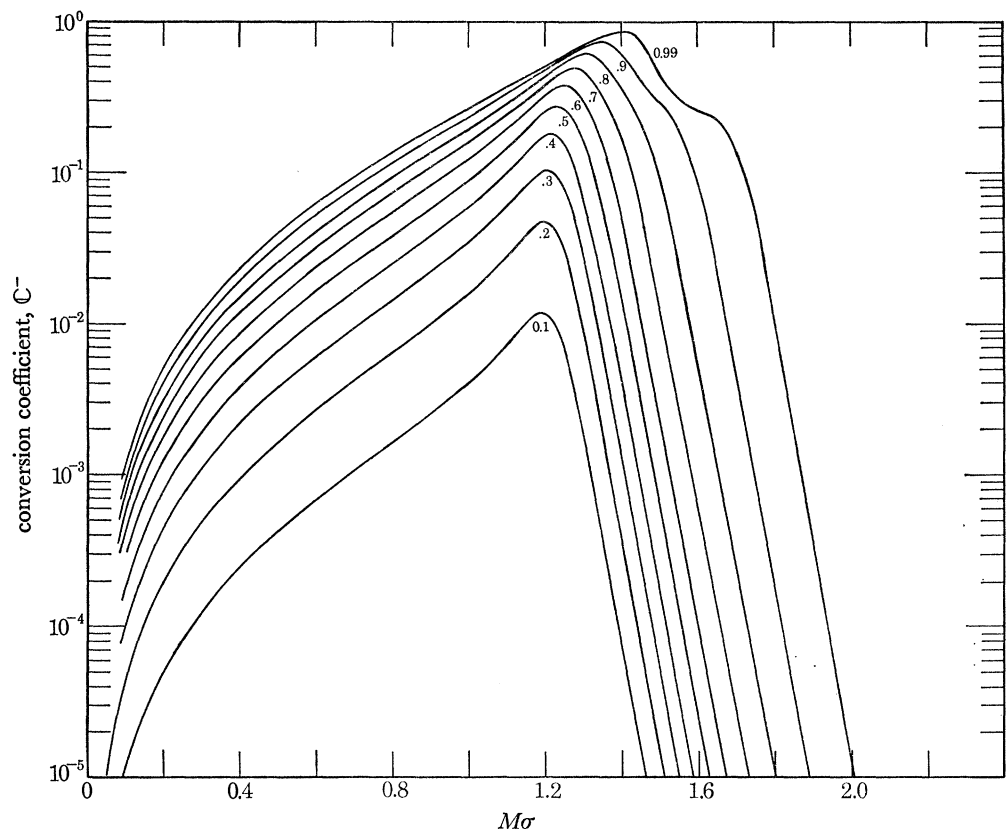


FIGURE 10. The conversion coefficient C^- for the odd-parity perturbations belonging to $l = 6$.
Each curve is labelled by the charge Q_* to which it belongs.

I wish to thank Dr S. Chandrasekhar, F.R.S., for making his results available to me prior to publication and for encouraging me throughout the research. I am grateful to Dr S. Detweiler and Dr J. Ipser for helpful discussions and comments. Finally, none of this research would have been possible without the constant support of my parents.

Funding for computer analysis was provided by a grant from the National Science Foundation under grant PHY 76-81102 with the University of Chicago.

REFERENCES

- Chandrasekhar, S. 1979 *Proc. R. Soc. Lond. A.*
Chandrasekhar, S. & Detweiler, S. 1975 *Proc. R. Soc. Lond. A* **344**, 441.
Cunningham, C., Price, R. & Moncrief, V. 1978 *Astrophys. J.* **224**, 643.
Matzner, R. 1976 *Phys. Rev. D* **14**, 3274.
Moncrief, V. 1974a *Phys. Rev. D* **9**, 2707.
Moncrief, V. 1974b *Phys. Rev. D* **10**, 1057.
Moncrief, V. 1975 *Phys. Rev. D* **12**, 1526.

PERTURBATIONS OF REISSNER-NORDSTRÖM BLACK HOLE 509

TABLE 1 (*a*). THE SCATTERING MATRIX OF PERTURBATIONS APPROPRIATE TO $l = 2$
FOR THE REISSNER-NORDSTRÖM BLACK HOLE WITH CHARGE $Q_* = 0.3M$
(In this and following tables 9.999 (-1) signifies 9.999×10^{-1})

$M\sigma$	\mathbb{R}_1	\mathbb{R}_2	δ_2^t	A_{12}^t	$\delta_2^{r,+}$	$A_{12}^{r,+}$	$\delta_2^{r,-}$	$A_{12}^{r,-}$
0.02	1.000	1.000	4.901	0.044	3.284	0.055	3.311	0.022
0.04	1.000	1.000	5.028	0.089	3.308	0.112	3.361	0.046
0.06	1.000	1.000	5.129	0.134	3.285	0.170	3.365	0.070
0.08	1.000	1.000	5.210	0.181	3.229	0.229	3.335	0.097
0.10	1.000	1.000	5.271	0.229	3.146	0.291	3.279	0.125
0.12	1.000	1.000	5.315	0.279	3.040	0.354	3.199	0.156
0.14	1.000	1.000	5.340	0.331	2.913	0.420	3.098	0.189
0.16	1.000	9.999 (-1)	5.348	0.386	2.765	0.488	2.977	0.224
0.18	1.000	9.997 (-1)	5.337	0.444	2.598	0.560	2.836	0.263
0.20	1.000	9.992 (-1)	5.307	0.505	2.412	0.636	2.676	0.307
0.22	9.999 (-1)	9.980 (-1)	5.257	0.572	2.205	0.718	2.495	0.355
0.24	9.998 (-1)	9.953 (-1)	5.185	0.645	1.976	0.805	2.292	0.411
0.26	9.995 (-1)	9.893 (-1)	5.088	0.726	1.724	0.902	2.065	0.474
0.28	9.989 (-1)	9.763 (-1)	4.964	0.818	1.444	1.009	1.812	0.549
0.30	9.977 (-1)	9.496 (-1)	4.808	0.924	1.133	1.130	1.527	0.638
0.32	9.951 (-1)	8.979 (-1)	4.616	1.047	0.787	1.268	1.206	0.745
0.34	9.898 (-1)	8.070 (-1)	4.386	1.187	0.404	1.424	0.848	0.868
0.36	9.792 (-1)	6.689 (-1)	4.123	1.338	0.271	1.590	0.457	1.003
0.38	9.585 (-1)	4.976 (-1)	3.839	1.482	0.836	1.750	0.047	1.131
0.40	9.201 (-1)	3.296 (-1)	3.557	1.595	0.403	1.878	5.922	1.227
0.42	8.529 (-1)	1.980 (-1)	3.297	1.653	0.991	1.951	5.535	1.270
0.44	7.468 (-1)	1.113 (-1)	3.067	1.648	0.612	1.962	5.180	1.249
0.46	6.022 (-1)	6.026 (-2)	2.870	1.585	0.265	1.915	4.858	1.171
0.48	4.394 (-1)	3.205 (-2)	2.699	1.483	0.946	1.828	4.563	1.054
0.50	2.902 (-1)	1.694 (-2)	2.552	1.365	0.650	1.726	4.292	0.921
0.52	1.768 (-1)	8.954 (-3)	2.423	1.250	0.374	1.625	4.039	0.790
0.54	1.020 (-1)	4.745 (-3)	2.309	1.146	0.113	1.538	3.802	0.672
0.56	5.694 (-2)	2.525 (-3)	2.207	1.058	0.865	1.465	3.577	0.570
0.58	3.128 (-2)	1.350 (-3)	2.115	0.984	0.627	1.406	3.362	0.481
0.60	1.705 (-2)	7.248 (-4)	2.032	0.922	0.398	1.359	3.156	0.404
0.62	9.281 (-3)	3.910 (-4)	1.955	0.869	0.216	1.321	2.957	0.337
0.64	5.054 (-3)	2.119 (-4)	1.885	0.823	0.161	1.290	2.765	0.277
0.66	2.759 (-3)	1.153 (-4)	1.820	0.783	0.753	1.265	2.579	0.224
0.68	1.510 (-3)	6.301 (-5)	1.760	0.748	0.549	1.245	2.397	0.175
0.70	8.287 (-4)	3.456 (-5)	1.703	0.716	0.350	1.228	2.220	0.130
0.72	4.563 (-4)	1.902 (-5)	1.651	0.688	0.155	1.215	2.046	0.088
0.74	2.520 (-4)	1.050 (-5)	1.602	0.662	0.963	1.204	1.877	0.049
0.76	1.396 (-4)	5.817 (-6)	1.556	0.638	0.775	1.195	1.710	0.012
0.78	7.752 (-5)	3.232 (-6)	1.513	0.617	0.591	1.187	1.546	6.260
0.80	4.317 (-5)	1.801 (-6)	1.472	0.597	0.409	1.182	1.385	6.227
0.82	2.410 (-5)	1.006 (-6)	1.433	0.578	0.229	1.177	1.227	6.196
0.84	1.349 (-5)	5.635 (-7)	1.396	0.561	0.052	1.174	1.070	6.166
0.86	7.563 (-6)	3.164 (-7)	1.362	0.545	0.161	1.172	0.916	6.137
0.88	4.251 (-6)	1.780 (-7)	1.329	0.529	0.989	1.171	0.763	6.109
0.90	2.394 (-6)	1.004 (-7)	1.297	0.515	0.818	1.170	0.612	6.083

TABLE 1 (b). THE SCATTERING MATRIX OF PERTURBATIONS APPROPRIATE TO $l = 3$
FOR THE REISSNER-NORDSTRÖM BLACK HOLE WITH CHARGE $Q_* = 0.3M$

$M\sigma$	\mathbb{R}_1	\mathbb{R}_2	δ_2^t	A_{12}^t	δ_2^{r+}	A_{12}^{r+}	δ_2^{r-}	A_{12}^{r-}
0.04	1.000	1.000	0.481	0.041	0.343	0.043	0.356	0.025
0.06	1.000	1.000	0.638	0.062	0.355	0.065	0.375	0.037
0.08	1.000	1.000	0.786	0.084	0.356	0.088	0.382	0.051
0.10	1.000	1.000	0.921	0.105	0.339	0.111	0.372	0.065
0.12	1.000	1.000	1.041	0.127	0.305	0.134	0.344	0.079
0.14	1.000	1.000	1.148	0.150	0.254	0.159	0.301	0.094
0.16	1.000	1.000	1.241	0.173	0.189	0.184	0.242	0.109
0.18	1.000	1.000	1.321	0.196	0.110	0.209	0.170	0.126
0.20	1.000	1.000	1.387	0.221	0.017	0.235	0.084	0.143
0.22	1.000	1.000	1.440	0.245	6.195	0.262	6.268	0.161
0.24	1.000	1.000	1.480	0.271	6.078	0.290	6.157	0.179
0.26	1.000	1.000	1.507	0.298	5.948	0.320	6.034	0.199
0.28	1.000	1.000	1.522	0.326	5.807	0.350	5.900	0.220
0.30	1.000	1.000	1.524	0.354	5.654	0.381	5.753	0.242
0.32	1.000	1.000	1.514	0.385	5.489	0.414	5.595	0.266
0.34	1.000	9.999 (-1)	1.490	0.416	5.312	0.449	5.425	0.291
0.36	1.000	9.999 (-1)	1.453	0.450	5.123	0.485	5.242	0.319
0.38	1.000	9.997 (-1)	1.402	0.486	4.921	0.524	5.046	0.348
0.40	9.999 (-1)	9.994 (-1)	1.337	0.524	4.705	0.565	4.837	0.380
0.42	9.999 (-1)	9.987 (-1)	1.257	0.566	4.474	0.610	4.613	0.416
0.44	9.997 (-1)	9.972 (-1)	1.160	0.612	4.228	0.659	4.374	0.455
0.46	9.994 (-1)	9.942 (-1)	1.044	0.662	3.965	0.713	4.117	0.500
0.48	9.988 (-1)	9.879 (-1)	0.908	0.720	3.681	0.773	3.840	0.551
0.50	9.975 (-1)	9.754 (-1)	0.749	0.785	3.375	0.842	3.540	0.611
0.52	9.949 (-1)	9.509 (-1)	0.562	0.862	3.042	0.922	3.214	0.682
0.54	9.898 (-1)	9.052 (-1)	0.344	0.951	2.678	1.015	2.857	0.765
0.56	9.797 (-1)	8.261 (-1)	0.092	1.053	2.281	1.120	2.466	0.862
0.58	9.605 (-1)	7.044 (-1)	6.091	1.164	1.852	1.234	2.044	0.966
0.60	9.249 (-1)	5.462 (-1)	5.784	1.269	1.402	1.343	1.600	1.066
0.62	8.628 (-1)	3.798 (-1)	5.472	1.348	0.946	1.426	1.151	1.139
0.64	7.637 (-1)	2.387 (-1)	5.175	1.381	0.506	1.462	0.717	1.167
0.66	6.256 (-1)	1.391 (-1)	4.904	1.361	0.093	1.446	0.311	1.142
0.68	4.649 (-1)	7.722 (-2)	4.664	1.297	5.994	1.386	6.218	1.072
0.70	3.123 (-1)	4.176 (-2)	4.453	1.209	5.641	1.301	5.872	0.978
0.72	1.926 (-1)	2.230 (-2)	4.265	1.115	5.312	1.211	5.550	0.879
0.74	1.118 (-1)	1.185 (-2)	4.099	1.028	5.005	1.128	5.249	0.787
0.76	6.254 (-2)	6.296 (-3)	3.948	0.952	4.714	1.056	4.965	0.706
0.78	3.429 (-2)	3.349 (-3)	3.812	0.889	4.438	0.996	4.695	0.637
0.80	1.862 (-2)	1.786 (-3)	3.687	0.835	4.173	0.947	4.437	0.578
0.82	1.007 (-2)	9.554 (-4)	3.572	0.789	3.918	0.905	4.189	0.527
0.84	5.447 (-3)	5.127 (-4)	3.465	0.750	3.673	0.870	3.949	0.483
0.86	2.949 (-3)	2.760 (-4)	3.365	0.716	3.434	0.840	3.718	0.444
0.88	1.600 (-3)	1.490 (-4)	3.272	0.686	3.203	0.814	3.493	0.409
0.90	8.701 (-4)	8.072 (-5)	3.185	0.659	2.978	0.791	3.274	0.377
0.92	4.744 (-4)	4.384 (-5)	3.103	0.635	2.758	0.771	3.060	0.348
0.94	2.593 (-4)	2.388 (-5)	3.025	0.613	2.542	0.753	2.851	0.321
0.96	1.421 (-4)	1.304 (-5)	2.952	0.593	2.332	0.738	2.647	0.296
0.98	7.806 (-5)	7.139 (-6)	2.882	0.574	2.125	0.723	2.447	0.273
1.00	4.298 (-5)	3.918 (-6)	2.816	0.557	1.922	0.710	2.251	0.251
1.02	2.372 (-5)	2.155 (-6)	2.753	0.541	1.723	0.699	2.058	0.230
1.04	1.312 (-5)	1.188 (-6)	2.693	0.526	1.527	0.688	1.868	0.210
1.06	7.273 (-6)	6.564 (-7)	2.636	0.513	1.334	0.678	1.682	0.192
1.08	4.039 (-6)	3.634 (-7)	2.582	0.499	1.143	0.670	1.498	0.174
1.10	2.248 (-6)	2.016 (-7)	2.529	0.487	0.956	0.662	1.316	0.157

TABLE 1 (c). THE SCATTERING MATRIX OF PERTURBATIONS APPROPRIATE TO $l = 6$
FOR THE REISSNER–NORDSTRÖM BLACK HOLE WITH CHARGE $Q_* = 0.3M$

$M\sigma$	R_1	R_2	δ_2^t	A_{12}^t	δ_2^{r+}	A_{12}^{r+}	δ_2^{r-}	A_{12}^{r-}
0.06	1.000	1.000	4.650	0.023	1.746	0.020	1.749	0.016
0.08	1.000	1.000	5.324	0.030	2.682	0.025	2.685	0.020
0.10	1.000	1.000	6.198	0.037	4.027	0.030	4.031	0.024
0.12	1.000	1.000	0.115	0.044	4.033	0.036	4.038	0.029
0.14	1.000	1.000	0.302	0.052	4.024	0.043	4.029	0.034
0.16	1.000	1.000	0.480	0.059	4.007	0.049	4.013	0.039
0.18	1.000	1.000	0.649	0.067	3.984	0.056	3.991	0.045
0.20	1.000	1.000	0.810	0.075	3.957	0.063	3.965	0.050
0.22	1.000	1.000	0.943	0.083	3.886	0.069	3.894	0.056
0.24	1.000	1.000	1.093	0.091	3.860	0.076	3.869	0.061
0.26	1.000	1.000	1.233	0.099	3.825	0.083	3.835	0.067
0.28	1.000	1.000	1.364	0.107	3.782	0.090	3.793	0.073
0.30	1.000	1.000	1.486	0.115	3.732	0.097	3.743	0.079
0.32	1.000	1.000	1.599	0.123	3.674	0.104	3.686	0.085
0.34	1.000	1.000	1.704	0.131	3.609	0.112	3.622	0.091
0.36	1.000	1.000	1.800	0.140	3.537	0.119	3.551	0.097
0.38	1.000	1.000	1.889	0.149	3.459	0.127	3.473	0.104
0.40	1.000	1.000	1.970	0.157	3.374	0.135	3.389	0.110
0.42	1.000	1.000	2.044	0.166	3.283	0.143	3.299	0.117
0.44	1.000	1.000	2.110	0.175	3.186	0.151	3.202	0.124
0.46	1.000	1.000	2.170	0.184	3.083	0.159	3.100	0.131
0.48	1.000	1.000	2.222	0.193	2.973	0.168	2.992	0.138
0.50	1.000	1.000	2.268	0.203	2.858	0.176	2.877	0.146
0.52	1.000	1.000	2.307	0.213	2.738	0.185	2.757	0.153
0.54	1.000	1.000	2.339	0.222	2.611	0.194	2.631	0.161
0.56	1.000	1.000	2.365	0.232	2.479	0.203	2.500	0.169
0.58	1.000	1.000	2.384	0.243	2.341	0.213	2.362	0.177
0.60	1.000	1.000	2.396	0.253	2.197	0.223	2.220	0.186
0.62	1.000	1.000	2.402	0.264	2.047	0.233	2.071	0.195
0.64	1.000	1.000	2.402	0.275	1.892	0.243	1.916	0.204
0.66	1.000	1.000	2.395	0.286	1.731	0.254	1.756	0.213
0.68	1.000	1.000	2.382	0.298	1.564	0.265	1.590	0.223
0.70	1.000	1.000	2.362	0.310	1.392	0.276	1.418	0.233
0.72	1.000	1.000	2.335	0.322	1.213	0.287	1.240	0.243
0.74	1.000	1.000	2.302	0.334	1.028	0.299	1.056	0.254
0.76	1.000	1.000	2.262	0.347	0.838	0.312	0.866	0.265
0.78	1.000	1.000	2.216	0.361	0.640	0.325	0.670	0.277
0.80	1.000	1.000	2.162	0.375	0.427	0.338	0.467	0.289
0.82	1.000	1.000	2.101	0.389	0.227	0.352	0.258	0.302
0.84	1.000	1.000	2.033	0.405	0.010	0.367	0.041	0.315
0.86	1.000	1.000	1.957	0.420	6.069	0.382	6.101	0.329
0.88	1.000	1.000	1.873	0.437	5.837	0.398	5.871	0.344

TABLE 1 (c) (*continued*)

$M\sigma$	R_1	R_2	δ_2^t	A_{12}^t	$\delta_2^{r,+}$	$A_{12}^{r,+}$	$\delta_2^{r,-}$	$A_{12}^{r,-}$
0.90	1.000	1.000	1.782	0.454	5.598	0.415	5.632	0.360
0.92	1.000	1.000	1.681	0.473	5.351	0.433	5.386	0.377
0.94	1.000	9.999 (-1)	1.572	0.492	5.096	0.452	5.131	0.394
0.96	1.000	9.999 (-1)	1.454	0.513	4.831	0.472	4.868	0.413
0.98	9.999 (-1)	9.997 (-1)	1.326	0.535	4.557	0.494	4.594	0.434
1.00	9.999 (-1)	9.995 (-1)	1.187	0.559	4.273	0.517	4.311	0.456
1.02	9.998 (-1)	9.989 (-1)	1.036	0.585	3.977	0.543	4.016	0.480
1.04	9.996 (-1)	9.979 (-1)	0.873	0.614	3.670	0.571	3.709	0.507
1.06	9.992 (-1)	9.957 (-1)	0.695	0.646	3.348	0.603	3.388	0.538
1.08	9.983 (-1)	9.916 (-1)	0.501	0.682	3.010	0.639	3.051	0.572
1.10	9.967 (-1)	9.835 (-1)	0.289	0.723	2.654	0.680	2.696	0.612
1.12	9.936 (-1)	9.681 (-1)	0.055	0.771	2.277	0.727	2.320	0.659
1.14	9.875 (-1)	9.392 (-1)	6.079	0.828	1.875	0.784	1.918	0.714
1.16	9.758 (-1)	8.877 (-1)	5.790	0.894	1.444	0.849	1.488	0.778
1.18	9.541 (-1)	8.024 (-1)	5.470	0.968	0.982	0.923	1.026	0.850
1.20	9.146 (-1)	6.765 (-1)	5.121	1.044	0.491	0.998	0.537	0.925
1.22	8.472 (-1)	5.194 (-1)	4.754	1.108	6.265	1.063	0.028	0.988
1.24	7.421 (-1)	3.591 (-1)	4.385	1.145	5.755	1.099	5.802	1.023
1.26	5.997 (-1)	2.256 (-1)	4.031	1.142	5.261	1.096	5.308	1.018
1.28	4.389 (-1)	1.318 (-1)	3.705	1.101	4.793	1.055	4.841	0.976
1.30	2.906 (-1)	7.355 (-2)	3.408	1.038	4.356	0.991	4.405	0.912
1.32	1.770 (-1)	3.996 (-2)	3.139	0.968	3.947	0.921	3.997	0.840
1.34	1.017 (-1)	2.141 (-2)	2.894	0.902	3.562	0.854	3.613	0.772
1.36	5.635 (-2)	1.139 (-2)	2.671	0.844	3.199	0.796	3.250	0.713
1.38	3.062 (-2)	6.050 (-3)	2.464	0.795	2.852	0.747	2.904	0.662
1.40	1.647 (-2)	3.212 (-3)	2.271	0.753	2.521	0.705	2.574	0.619
1.42	8.821 (-3)	1.707 (-3)	2.091	0.718	2.201	0.670	2.255	0.583
1.44	4.717 (-3)	9.086 (-4)	1.921	0.688	1.893	0.639	1.947	0.551
1.46	2.523 (-3)	4.844 (-4)	1.761	0.661	1.594	0.612	1.649	0.523
1.48	1.351 (-3)	2.588 (-4)	1.609	0.638	1.304	0.589	1.360	0.498
1.50	7.245 (-4)	1.385 (-4)	1.464	0.617	1.021	0.568	1.078	0.476
1.52	3.892 (-4)	7.426 (-5)	1.326	0.598	0.745	0.548	0.803	0.455
1.54	2.094 (-4)	3.989 (-5)	1.195	0.581	0.476	0.531	0.534	0.436
1.56	1.129 (-4)	2.147 (-5)	1.068	0.565	0.212	0.515	0.271	0.419
1.58	6.095 (-5)	1.158 (-5)	0.947	0.550	6.237	0.500	0.013	0.403
1.60	3.297 (-5)	6.253 (-6)	0.831	0.536	5.983	0.486	6.043	0.388
1.62	1.786 (-5)	3.383 (-6)	0.719	0.523	5.734	0.473	5.795	0.374
1.64	9.695 (-6)	1.834 (-6)	0.611	0.511	5.490	0.461	5.551	0.360
1.66	5.270 (-6)	9.953 (-7)	0.507	0.500	5.249	0.449	5.312	0.348
1.68	2.870 (-6)	5.411 (-7)	0.407	0.490	5.012	0.439	5.076	0.336
1.70	1.565 (-6)	2.947 (-7)	0.310	0.480	4.779	0.428	4.843	0.324

PERTURBATIONS OF REISSNER–NORDSTRÖM BLACK HOLE 513

TABLE 2 (a). THE SCATTERING MATRIX OF PERTURBATIONS APPROPRIATE TO $l = 2$
FOR THE REISSNER–NORDSTRÖM BLACK HOLE WITH CHARGE $Q_* = 0.5M$

$M\sigma$	\mathbb{R}_1	\mathbb{R}_2	δ_2^t	A_{12}^t	$\delta_2^{r,+}$	$A_{12}^{r,+}$	$\delta_2^{r,-}$	$A_{12}^{r,-}$
0.02	1.000	1.000	4.904	0.050	3.287	0.058	3.313	0.025
0.04	1.000	1.000	5.035	0.101	3.313	0.117	3.366	0.051
0.06	1.000	1.000	5.140	0.154	3.293	0.178	3.372	0.079
0.08	1.000	1.000	5.224	0.207	3.239	0.240	3.346	0.108
0.10	1.000	1.000	5.289	0.262	3.160	0.305	3.292	0.140
0.12	1.000	1.000	5.336	0.319	3.057	0.372	3.216	0.173
0.14	1.000	1.000	5.366	0.378	2.933	0.441	3.118	0.210
0.16	1.000	9.999 (-1)	5.377	0.440	2.789	0.514	3.001	0.250
0.18	1.000	9.997 (-1)	5.371	0.505	2.626	0.590	2.864	0.293
0.20	1.000	9.993 (-1)	5.345	0.574	2.443	0.670	2.708	0.340
0.22	1.000	9.984 (-1)	5.300	0.649	2.241	0.756	2.531	0.393
0.24	9.999 (-1)	9.961 (-1)	5.233	0.729	2.018	0.848	2.334	0.453
0.26	9.998 (-1)	9.911 (-1)	5.143	0.819	1.772	0.949	2.113	0.522
0.28	9.995 (-1)	9.804 (-1)	5.026	0.919	1.499	1.061	1.867	0.602
0.30	9.989 (-1)	9.580 (-1)	4.879	1.033	1.197	1.188	1.591	0.696
0.32	9.977 (-1)	9.142 (-1)	4.698	1.165	0.862	1.332	1.280	0.808
0.34	9.952 (-1)	8.351 (-1)	4.479	1.317	0.489	1.495	0.933	0.940
0.36	9.902 (-1)	7.099 (-1)	4.224	1.483	0.082	1.675	0.551	1.087
0.38	9.803 (-1)	5.453 (-1)	3.945	1.652	5.934	1.856	0.145	1.237
0.40	9.613 (-1)	3.731 (-1)	3.661	1.800	5.499	2.016	6.018	1.366
0.42	9.260 (-1)	2.301 (-1)	3.394	1.903	5.081	2.132	5.625	1.450
0.44	8.643 (-1)	1.316 (-1)	3.155	1.945	4.693	2.186	5.261	1.474
0.46	7.660 (-1)	7.201 (-2)	2.949	1.923	4.337	2.177	4.930	1.433
0.48	6.290 (-1)	3.853 (-2)	2.772	1.846	4.011	2.112	4.628	1.338
0.50	4.695 (-1)	2.043 (-2)	2.618	1.730	3.710	2.009	4.351	1.204
0.52	3.174 (-1)	1.081 (-2)	2.484	1.598	3.429	1.889	4.094	1.054
0.54	1.974 (-1)	5.735 (-3)	2.366	1.468	3.164	1.772	3.852	0.907
0.56	1.157 (-1)	3.053 (-3)	2.261	1.351	2.912	1.668	3.624	0.773
0.58	6.545 (-2)	1.632 (-3)	2.166	1.251	2.671	1.580	3.406	0.655
0.60	3.629 (-2)	8.766 (-4)	2.079	1.165	2.440	1.507	3.198	0.553
0.62	1.994 (-2)	4.730 (-4)	2.001	1.094	2.216	1.448	2.997	0.464
0.64	1.092 (-2)	2.563 (-4)	1.928	1.032	2.000	1.399	2.803	0.386
0.66	5.977 (-3)	1.395 (-4)	1.861	0.979	1.789	1.358	2.615	0.316
0.68	3.278 (-3)	7.622 (-5)	1.800	0.932	1.584	1.324	2.432	0.254
0.70	1.802 (-3)	4.180 (-5)	1.742	0.891	1.384	1.295	2.254	0.196
0.72	9.931 (-4)	2.301 (-5)	1.688	0.854	1.187	1.270	2.079	0.143
0.74	5.489 (-4)	1.270 (-5)	1.638	0.821	0.995	1.249	1.909	0.094
0.76	3.042 (-4)	7.038 (-6)	1.590	0.791	0.806	1.231	1.741	0.048
0.78	1.691 (-4)	3.911 (-6)	1.546	0.763	0.621	1.215	1.577	0.005
0.80	9.420 (-5)	2.179 (-6)	1.504	0.738	0.438	1.202	1.415	6.248
0.82	5.261 (-5)	1.217 (-6)	1.465	0.714	0.258	1.190	1.255	6.209
0.84	2.946 (-5)	6.819 (-7)	1.427	0.692	0.081	1.180	1.098	6.172
0.86	1.653 (-5)	3.829 (-7)	1.391	0.672	6.189	1.171	0.943	6.136
0.88	9.295 (-6)	2.155 (-7)	1.358	0.653	6.016	1.164	0.790	6.103
0.90	5.238 (-6)	1.215 (-7)	1.326	0.635	5.845	1.157	0.639	6.070
0.92	2.957 (-6)	6.870 (-8)	1.295	0.618	5.676	1.152	0.489	6.039
0.94	1.673 (-6)	3.891 (-8)	1.266	0.602	5.508	1.147	0.341	6.008
0.96	9.477 (-7)	2.208 (-8)	1.238	0.587	5.343	1.143	0.194	5.979
0.98	5.379 (-7)	1.255 (-8)	1.212	0.573	5.178	1.140	0.049	5.951
1.00	3.058 (-7)	7.148 (-9)	1.186	0.559	5.016	1.138	6.188	5.923

TABLE 2(b). THE SCATTERING MATRIX OF PERTURBATIONS APPROPRIATE TO $l = 3$
FOR THE REISSNER–NORDSTRÖM BLACK HOLE WITH CHARGE $Q_* = 0.5M$

$M\sigma$	\mathbb{R}_1	\mathbb{R}_2	δ_2^t	A_{12}^t	$\delta_2^{r,+}$	$A_{12}^{r,+}$	$\delta_2^{r,-}$	$A_{12}^{r,-}$
0.04	1.000	1.000	0.488	0.052	0.348	0.049	0.361	0.030
0.06	1.000	1.000	0.650	0.079	0.362	0.073	0.382	0.046
0.08	1.000	1.000	0.801	0.106	0.365	0.099	0.392	0.062
0.10	1.000	1.000	0.940	0.133	0.351	0.125	0.384	0.079
0.12	1.000	1.000	1.064	0.161	0.320	0.152	0.359	0.097
0.14	1.000	1.000	1.175	0.189	0.272	0.180	0.319	0.115
0.16	1.000	1.000	1.272	0.218	0.210	0.208	0.263	0.134
0.18	1.000	1.000	1.355	0.248	0.134	0.238	0.193	0.154
0.20	1.000	1.000	1.425	0.278	0.044	0.268	0.110	0.175
0.22	1.000	1.000	1.482	0.310	6.225	0.299	0.015	0.197
0.24	1.000	1.000	1.526	0.342	6.111	0.331	6.190	0.220
0.26	1.000	1.000	1.558	0.375	5.985	0.364	6.071	0.244
0.28	1.000	1.000	1.577	0.410	5.847	0.399	5.940	0.269
0.30	1.000	1.000	1.584	0.445	5.698	0.435	5.798	0.296
0.32	1.000	1.000	1.578	0.483	5.537	0.473	5.643	0.325
0.34	1.000	1.000	1.559	0.522	5.365	0.513	5.477	0.355
0.36	1.000	9.999 (-1)	1.527	0.563	5.180	0.555	5.299	0.388
0.38	1.000	9.998 (-1)	1.482	0.607	4.983	0.599	5.109	0.423
0.40	1.000	9.996 (-1)	1.423	0.654	4.773	0.647	4.905	0.462
0.42	1.000	9.991 (-1)	1.349	0.704	4.548	0.698	4.687	0.503
0.44	9.999 (-1)	9.980 (-1)	1.259	0.758	4.309	0.753	4.455	0.550
0.46	9.998 (-1)	9.958 (-1)	1.151	0.818	4.053	0.814	4.205	0.601
0.48	9.996 (-1)	9.912 (-1)	1.025	0.885	3.779	0.882	3.937	0.660
0.50	9.991 (-1)	9.819 (-1)	0.876	0.960	3.483	0.958	3.648	0.727
0.52	9.982 (-1)	9.637 (-1)	0.702	1.047	3.162	1.046	3.334	0.806
0.54	9.963 (-1)	9.291 (-1)	0.499	1.148	2.813	1.148	2.992	0.899
0.56	9.926 (-1)	8.669 (-1)	0.263	1.264	2.432	1.266	2.617	1.008
0.58	9.854 (-1)	7.654 (-1)	6.277	1.395	2.018	1.399	2.209	1.131
0.60	9.715 (-1)	6.223 (-1)	5.979	1.532	1.576	1.537	1.774	1.260
0.62	9.458 (-1)	4.559 (-1)	5.667	1.657	1.121	1.664	1.326	1.378
0.64	8.997 (-1)	3.001 (-1)	5.362	1.748	0.672	1.757	0.883	1.461
0.66	8.226 (-1)	1.808 (-1)	5.078	1.786	0.245	1.797	0.463	1.492
0.68	7.069 (-1)	1.026 (-1)	4.823	1.766	6.132	1.778	0.073	1.464
0.70	5.577 (-1)	5.615 (-2)	4.599	1.694	5.766	1.708	5.997	1.385
0.72	3.985 (-1)	3.018 (-2)	4.400	1.590	5.426	1.606	5.664	1.273
0.74	2.591 (-1)	1.609 (-2)	4.224	1.474	5.109	1.492	5.353	1.151
0.76	1.564 (-1)	8.559 (-3)	4.066	1.363	4.810	1.383	5.061	1.032
0.78	8.987 (-2)	4.555 (-3)	3.923	1.264	4.527	1.286	4.784	0.926
0.80	5.014 (-2)	2.429 (-3)	3.792	1.180	4.257	1.204	4.521	0.835
0.82	2.754 (-2)	1.299 (-3)	3.672	1.108	3.997	1.134	4.268	0.757
0.84	1.502 (-2)	6.969 (-4)	3.561	1.048	3.747	1.076	4.024	0.689
0.86	8.171 (-3)	3.750 (-4)	3.458	0.996	3.505	1.026	3.788	0.630
0.88	4.445 (-3)	2.024 (-4)	3.361	0.950	3.270	0.983	3.560	0.578
0.90	2.421 (-3)	1.095 (-4)	3.270	0.910	3.042	0.945	3.338	0.531
0.92	1.321 (-3)	5.947 (-5)	3.185	0.875	2.819	0.912	3.122	0.489
0.94	7.228 (-4)	3.237 (-5)	3.105	0.843	2.601	0.882	2.910	0.450
0.96	3.963 (-4)	1.767 (-5)	3.029	0.814	2.388	0.856	2.704	0.414
0.98	2.178 (-4)	9.667 (-6)	2.958	0.787	2.180	0.831	2.502	0.381
1.00	1.200 (-4)	5.303 (-6)	2.889	0.763	1.975	0.809	2.303	0.350
1.02	6.625 (-5)	2.915 (-6)	2.825	0.740	1.774	0.789	2.108	0.320
1.04	3.666 (-5)	1.606 (-6)	2.763	0.719	1.576	0.771	1.917	0.293
1.06	2.032 (-5)	8.869 (-7)	2.704	0.699	1.381	0.754	1.729	0.267
1.08	1.129 (-5)	4.907 (-7)	2.648	0.681	1.189	0.738	1.543	0.242
1.10	6.286 (-6)	2.720 (-7)	2.594	0.664	1.000	0.723	1.360	0.218

PERTURBATIONS OF REISSNER-NORDSTRÖM BLACK HOLE 515

TABLE 2(c). THE SCATTERING MATRIX OF PERTURBATIONS APPROPRIATE TO $l = 6$
FOR THE REISSNER-NORDSTRÖM BLACK HOLE WITH CHARGE $Q_* = 0.5M$

$M\sigma$	\mathbb{R}_1	\mathbb{R}_2	δ_2^t	A_{12}^t	$\delta_2^{r,+}$	$A_{12}^{r,+}$	$\delta_2^{r,-}$	$A_{12}^{r,-}$
0.06	1.000	1.000	4.663	0.035	1.753	0.028	1.755	0.025
0.08	1.000	1.000	5.343	0.045	2.693	0.034	2.696	0.029
0.10	1.000	1.000	6.222	0.055	4.041	0.041	4.044	0.034
0.12	1.000	1.000	0.144	0.066	4.050	0.049	4.055	0.042
0.14	1.000	1.000	0.335	0.077	4.043	0.058	4.049	0.049
0.16	1.000	1.000	0.518	0.089	4.029	0.066	4.035	0.057
0.18	1.000	1.000	0.691	0.100	4.010	0.076	4.017	0.065
0.20	1.000	1.000	0.857	0.112	3.986	0.085	3.993	0.072
0.22	1.000	1.000	0.994	0.124	3.917	0.094	3.926	0.080
0.24	1.000	1.000	1.149	0.135	3.894	0.103	3.903	0.088
0.26	1.000	1.000	1.294	0.147	3.863	0.113	3.873	0.097
0.28	1.000	1.000	1.429	0.159	3.823	0.122	3.834	0.105
0.30	1.000	1.000	1.556	0.171	3.776	0.132	3.787	0.114
0.32	1.000	1.000	1.674	0.184	3.721	0.142	3.733	0.122
0.34	1.000	1.000	1.783	0.196	3.660	0.152	3.673	0.131
0.36	1.000	1.000	1.884	0.209	3.591	0.162	3.605	0.140
0.38	1.000	1.000	1.978	0.221	3.517	0.173	3.531	0.150
0.40	1.000	1.000	2.064	0.234	3.435	0.184	3.450	0.159
0.42	1.000	1.000	2.142	0.247	3.348	0.195	3.364	0.169
0.44	1.000	1.000	2.214	0.261	3.254	0.206	3.271	0.179
0.46	1.000	1.000	2.278	0.274	3.155	0.217	3.172	0.189
0.48	1.000	1.000	2.335	0.288	3.050	0.229	3.068	0.200
0.50	1.000	1.000	2.386	0.302	2.939	0.241	2.958	0.210
0.52	1.000	1.000	2.430	0.316	2.822	0.253	2.842	0.221
0.54	1.000	1.000	2.467	0.331	2.700	0.266	2.720	0.232
0.56	1.000	1.000	2.498	0.345	2.571	0.278	2.593	0.244
0.58	1.000	1.000	2.522	0.360	2.438	0.291	2.460	0.256
0.60	1.000	1.000	2.540	0.376	2.299	0.305	2.321	0.268
0.62	1.000	1.000	2.552	0.392	2.154	0.319	2.177	0.281
0.64	1.000	1.000	2.557	0.408	2.003	0.333	2.027	0.294
0.66	1.000	1.000	2.556	0.424	1.847	0.347	1.872	0.307
0.68	1.000	1.000	2.549	0.441	1.685	0.362	1.711	0.321
0.70	1.000	1.000	2.535	0.458	1.518	0.378	1.544	0.335
0.72	1.000	1.000	2.515	0.476	1.345	0.394	1.372	0.350
0.74	1.000	1.000	2.488	0.494	1.166	0.410	1.194	0.365
0.76	1.000	1.000	2.455	0.513	0.981	0.427	1.009	0.381
0.78	1.000	1.000	2.415	0.532	0.790	0.445	0.819	0.397
0.80	1.000	1.000	2.368	0.552	0.592	0.463	0.622	0.414
0.82	1.000	1.000	2.314	0.573	0.389	0.483	0.420	0.432
0.84	1.000	1.000	2.254	0.595	0.178	0.502	0.210	0.451
0.86	1.000	1.000	2.186	0.617	6.245	0.523	6.277	0.470
0.88	1.000	1.000	2.111	0.640	6.021	0.545	6.054	0.491

TABLE 2 (c) (*continued*)

$M\sigma$	\mathbb{R}_1	\mathbb{R}_2	δ_2^t	A_{12}^t	$\delta_2^{r,+}$	$A_{12}^{r,+}$	$\delta_2^{r,-}$	$A_{12}^{r,-}$
0.90	1.000	1.000	2.028	0.665	5.790	0.568	5.824	0.512
0.92	1.000	1.000	1.937	0.690	5.551	0.592	5.586	0.535
0.94	1.000	1.000	1.837	0.717	5.305	0.617	5.341	0.559
0.96	1.000	9.999 (-1)	1.729	0.746	5.050	0.644	5.087	0.585
0.98	1.000	9.999 (-1)	1.612	0.776	4.787	0.672	4.824	0.612
1.00	1.000	9.998 (-1)	1.485	0.808	4.514	0.703	4.552	0.642
1.02	1.000	9.995 (-1)	1.348	0.842	4.231	0.736	4.270	0.673
1.04	9.999 (-1)	9.990 (-1)	1.199	0.880	3.938	0.772	3.977	0.708
1.06	9.998 (-1)	9.981 (-1)	1.038	0.920	3.632	0.811	3.672	0.746
1.08	9.997 (-1)	9.962 (-1)	0.863	0.965	3.312	0.854	3.353	0.788
1.10	9.994 (-1)	9.925 (-1)	0.673	1.016	2.978	0.903	3.019	0.836
1.12	9.988 (-1)	9.854 (-1)	0.464	1.073	2.625	0.959	2.668	0.890
1.14	9.976 (-1)	9.717 (-1)	0.235	1.138	2.253	1.023	2.296	0.953
1.16	9.954 (-1)	9.460 (-1)	6.264	1.214	1.856	1.098	1.899	1.027
1.18	9.910 (-1)	9.000 (-1)	5.981	1.303	1.431	1.186	1.475	1.113
1.20	9.828 (-1)	8.225 (-1)	5.668	1.405	0.975	1.286	1.021	1.212
1.22	9.672 (-1)	7.052 (-1)	5.326	1.516	0.491	1.395	0.537	1.320
1.24	9.388 (-1)	5.535 (-1)	4.962	1.623	6.268	1.501	0.032	1.425
1.26	8.887 (-1)	3.918 (-1)	4.593	1.708	5.757	1.585	5.805	1.508
1.28	8.065 (-1)	2.513 (-1)	4.235	1.752	5.259	1.627	5.307	1.548
1.30	6.858 (-1)	1.492 (-1)	3.903	1.742	4.785	1.616	4.834	1.537
1.32	5.340 (-1)	8.415 (-2)	3.600	1.685	4.342	1.557	4.391	1.477
1.34	3.763 (-1)	4.605 (-2)	3.325	1.595	3.927	1.467	3.977	1.384
1.36	2.415 (-1)	2.479 (-2)	3.075	1.494	3.537	1.364	3.588	1.280
1.38	1.442 (-1)	1.324 (-2)	2.847	1.395	3.169	1.264	3.221	1.180
1.40	8.199 (-2)	7.050 (-3)	2.636	1.308	2.818	1.176	2.871	1.090
1.42	4.532 (-2)	3.751 (-3)	2.441	1.233	2.483	1.099	2.537	1.012
1.44	2.466 (-2)	1.997 (-3)	2.257	1.169	2.161	1.035	2.215	0.946
1.46	1.332 (-2)	1.065 (-3)	2.085	1.115	1.849	0.979	1.905	0.890
1.48	7.167 (-3)	5.687 (-4)	1.922	1.068	1.548	0.931	1.604	0.840
1.50	3.854 (-3)	3.042 (-4)	1.768	1.027	1.255	0.889	1.312	0.797
1.52	2.074 (-3)	1.631 (-4)	1.621	0.991	0.970	0.852	1.027	0.759
1.54	1.117 (-3)	8.755 (-5)	1.481	0.959	0.692	0.818	0.750	0.724
1.56	6.023 (-4)	4.710 (-5)	1.347	0.930	0.420	0.788	0.479	0.692
1.58	3.253 (-4)	2.538 (-5)	1.219	0.903	0.155	0.760	0.214	0.663
1.60	1.760 (-4)	1.370 (-5)	1.096	0.878	6.177	0.734	6.238	0.636
1.62	9.540 (-5)	7.409 (-6)	0.978	0.856	5.922	0.711	5.983	0.611
1.64	5.178 (-5)	4.013 (-6)	0.865	0.835	5.671	0.688	5.733	0.588
1.66	2.815 (-5)	2.177 (-6)	0.755	0.815	5.425	0.668	5.488	0.566
1.68	1.533 (-5)	1.183 (-6)	0.650	0.796	5.183	0.648	5.246	0.545
1.70	8.361 (-6)	6.439 (-7)	0.548	0.779	4.945	0.630	5.009	0.525

TABLE 3(a). THE SCATTERING MATRIX OF PERTURBATIONS APPROPRIATE TO $l = 2$
FOR THE REISSNER–NORDSTRÖM BLACK HOLE WITH CHARGE $Q_* = 0.7M$

$M\sigma$	\mathbb{R}_1	\mathbb{R}_2	$\delta_{\mathbb{R}_2}^t$	A_{12}^t	$\delta_{\mathbb{R}_2}^{r,+}$	$A_{12}^{r,+}$	$\delta_{\mathbb{R}_2}^{r,-}$	$A_{12}^{r,-}$
0.02	1.000	1.000	4.913	0.061	3.292	0.061	3.318	0.028
0.04	1.000	1.000	5.053	0.122	3.323	0.124	3.377	0.058
0.06	1.000	1.000	5.167	0.185	3.309	0.189	3.388	0.089
0.08	1.000	1.000	5.260	0.249	3.261	0.255	3.367	0.123
0.10	1.000	1.000	5.334	0.315	3.187	0.324	3.320	0.159
0.12	1.000	1.000	5.390	0.383	3.091	0.395	3.250	0.197
0.14	1.000	1.000	5.428	0.453	2.973	0.469	3.159	0.238
0.16	1.000	9.999 (-1)	5.449	0.526	2.837	0.547	3.048	0.283
0.18	1.000	9.998 (-1)	5.452	0.603	2.681	0.628	2.919	0.331
0.20	1.000	9.996 (-1)	5.436	0.683	2.507	0.714	2.771	0.384
0.22	1.000	9.989 (-1)	5.400	0.769	2.314	0.805	2.604	0.442
0.24	1.000	9.974 (-1)	5.345	0.862	2.100	0.902	2.417	0.508
0.26	9.999 (-1)	9.941 (-1)	5.267	0.962	1.866	1.009	2.208	0.581
0.28	9.999 (-1)	9.867 (-1)	5.164	1.073	1.607	1.126	1.974	0.666
0.30	9.997 (-1)	9.713 (-1)	5.033	1.198	1.321	1.257	1.714	0.765
0.32	9.994 (-1)	9.402 (-1)	4.870	1.340	1.003	1.405	1.422	0.882
0.34	9.988 (-1)	8.816 (-1)	4.671	1.504	0.651	1.575	1.095	1.019
0.36	9.976 (-1)	7.818 (-1)	4.434	1.688	0.261	1.765	0.731	1.178
0.38	9.950 (-1)	6.361 (-1)	4.166	1.886	6.124	1.970	0.336	1.351
0.40	9.900 (-1)	4.636 (-1)	3.881	2.081	5.689	2.172	6.209	1.522
0.42	9.803 (-1)	3.018 (-1)	3.603	2.248	5.261	2.346	5.804	1.665
0.44	9.620 (-1)	1.792 (-1)	3.347	2.368	4.856	2.473	5.424	1.761
0.46	9.283 (-1)	1.002 (-1)	3.123	2.430	4.483	2.542	5.076	1.798
0.48	8.699 (-1)	5.418 (-2)	2.929	2.429	4.142	2.549	4.759	1.774
0.50	7.767 (-1)	2.884 (-2)	2.763	2.372	3.827	2.498	4.469	1.693
0.52	6.457 (-1)	1.527 (-2)	2.617	2.265	3.536	2.398	4.201	1.563
0.54	4.901 (-1)	8.088 (-3)	2.490	2.125	3.263	2.266	3.951	1.400
0.56	3.376 (-1)	4.294 (-3)	2.377	1.971	3.004	2.119	3.716	1.224
0.58	2.137 (-1)	2.289 (-3)	2.275	1.821	2.758	1.976	3.493	1.052
0.60	1.272 (-1)	1.226 (-3)	2.183	1.686	2.522	1.848	3.280	0.894
0.62	7.276 (-2)	6.590 (-4)	2.099	1.569	2.295	1.738	3.076	0.755
0.64	4.071 (-2)	3.559 (-4)	2.023	1.469	2.075	1.645	2.878	0.633
0.66	2.253 (-2)	1.930 (-4)	1.952	1.383	1.862	1.567	2.688	0.526
0.68	1.241 (-2)	1.051 (-4)	1.886	1.310	1.654	1.501	2.502	0.431
0.70	6.828 (-3)	5.746 (-5)	1.825	1.246	1.452	1.444	2.322	0.345
0.72	3.760 (-3)	3.152 (-5)	1.769	1.190	1.254	1.395	2.146	0.268
0.74	2.074 (-3)	1.735 (-5)	1.715	1.140	1.061	1.352	1.974	0.197
0.76	1.147 (-3)	9.578 (-6)	1.666	1.095	0.871	1.314	1.805	0.132
0.78	6.356 (-4)	5.305 (-6)	1.619	1.054	0.684	1.281	1.640	0.070
0.80	3.531 (-4)	2.946 (-6)	1.575	1.017	0.501	1.250	1.478	0.013
0.82	1.966 (-4)	1.641 (-6)	1.533	0.983	0.321	1.223	1.318	6.242
0.84	1.097 (-4)	9.162 (-7)	1.494	0.951	0.143	1.199	1.160	6.190
0.86	6.139 (-5)	5.128 (-7)	1.456	0.922	6.251	1.176	1.005	6.141
0.88	3.441 (-5)	2.877 (-7)	1.421	0.895	6.078	1.156	0.852	6.095
0.90	1.933 (-5)	1.618 (-7)	1.387	0.869	5.907	1.137	0.701	6.050
0.92	1.088 (-5)	9.115 (-8)	1.355	0.845	5.738	1.120	0.552	6.007
0.94	6.134 (-6)	5.147 (-8)	1.324	0.823	5.571	1.104	0.404	5.965
0.96	3.465 (-6)	2.912 (-8)	1.295	0.802	5.406	1.089	0.258	5.925
0.98	1.960 (-6)	1.650 (-8)	1.267	0.782	5.242	1.076	0.113	5.886
1.00	1.111 (-6)	9.370 (-9)	1.241	0.763	5.080	1.063	6.253	5.849

TABLE 3 (b). THE SCATTERING MATRIX OF PERTURBATIONS APPROPRIATE TO $l = 3$
FOR THE REISSNER-NORDSTRÖM BLACK HOLE WITH CHARGE $Q_* = 0.7M$

$M\sigma$	\mathbb{R}_1	\mathbb{R}_2	δ_2^t	A_{12}^t	δ_2^{r+}	A_{12}^{r+}	δ_2^{r-}	A_{12}^{r-}
0.04	1.000	1.000	0.509	0.069	0.358	0.056	0.372	0.037
0.06	1.000	1.000	0.681	0.103	0.378	0.084	0.398	0.056
0.08	1.000	1.000	0.843	0.138	0.387	0.113	0.413	0.076
0.10	1.000	1.000	0.991	0.174	0.378	0.143	0.411	0.097
0.12	1.000	1.000	1.126	0.210	0.352	0.174	0.392	0.119
0.14	1.000	1.000	1.246	0.247	0.311	0.206	0.357	0.141
0.16	1.000	1.000	1.352	0.285	0.255	0.239	0.308	0.165
0.18	1.000	1.000	1.445	0.323	0.185	0.272	0.244	0.189
0.20	1.000	1.000	1.524	0.363	0.102	0.307	0.168	0.214
0.22	1.000	1.000	1.590	0.403	0.006	0.343	0.079	0.241
0.24	1.000	1.000	1.644	0.444	6.182	0.380	6.261	0.269
0.26	1.000	1.000	1.685	0.487	6.063	0.418	6.149	0.298
0.28	1.000	1.000	1.713	0.531	5.933	0.458	6.026	0.329
0.30	1.000	1.000	1.730	0.577	5.792	0.500	5.891	0.361
0.32	1.000	1.000	1.733	0.624	5.639	0.544	5.745	0.396
0.34	1.000	1.000	1.725	0.673	5.475	0.589	5.588	0.432
0.36	1.000	1.000	1.703	0.725	5.299	0.637	5.419	0.471
0.38	1.000	9.999 (-1)	1.669	0.779	5.112	0.688	5.238	0.512
0.40	1.000	9.998 (-1)	1.622	0.836	4.912	0.742	5.045	0.557
0.42	1.000	9.995 (-1)	1.560	0.897	4.700	0.800	4.839	0.606
0.44	1.000	9.990 (-1)	1.484	0.962	4.473	0.862	4.619	0.659
0.46	1.000	9.979 (-1)	1.392	1.032	4.232	0.929	4.384	0.717
0.48	9.999 (-1)	9.955 (-1)	1.282	1.109	3.974	1.003	4.133	0.781
0.50	9.998 (-1)	9.907 (-1)	1.154	1.194	3.697	1.085	3.863	0.854
0.52	9.997 (-1)	9.811 (-1)	1.003	1.289	3.400	1.178	3.571	0.938
0.54	9.994 (-1)	9.621 (-1)	0.827	1.398	3.077	1.284	3.256	1.035
0.56	9.987 (-1)	9.264 (-1)	0.621	1.523	2.726	1.407	2.911	1.148
0.58	9.975 (-1)	8.626 (-1)	0.382	1.666	2.342	1.548	2.534	1.280
0.60	9.951 (-1)	7.593 (-1)	0.110	1.828	1.926	1.707	2.124	1.430
0.62	9.904 (-1)	6.149 (-1)	6.094	2.000	1.483	1.877	1.688	1.591
0.64	9.814 (-1)	4.486 (-1)	5.782	2.165	1.028	2.040	1.239	1.745
0.66	9.645 (-1)	2.943 (-1)	5.475	2.302	0.579	2.175	0.797	1.870
0.68	9.337 (-1)	1.769 (-1)	5.191	2.391	0.153	2.262	0.377	1.948
0.70	8.801 (-1)	1.002 (-1)	4.937	2.421	6.040	2.290	6.271	1.967
0.72	7.936 (-1)	5.482 (-2)	4.712	2.392	5.674	2.259	5.912	1.927
0.74	6.691 (-1)	2.946 (-2)	4.513	2.309	5.335	2.175	5.579	1.834
0.76	5.166 (-1)	1.570 (-2)	4.336	2.187	5.018	2.051	5.268	1.701
0.78	3.618 (-1)	8.349 (-3)	4.177	2.045	4.719	1.908	4.976	1.548
0.80	2.320 (-1)	4.441 (-3)	4.033	1.902	4.436	1.763	4.699	1.394
0.82	1.390 (-1)	2.367 (-3)	3.901	1.770	4.165	1.630	4.435	1.252
0.84	7.973 (-2)	1.265 (-3)	3.780	1.655	3.906	1.513	4.182	1.126
0.86	4.456 (-2)	6.779 (-4)	3.668	1.556	3.655	1.413	3.938	1.017
0.88	2.457 (-2)	3.643 (-4)	3.563	1.472	3.413	1.327	3.703	0.922
0.90	1.346 (-2)	1.964 (-4)	3.465	1.399	3.178	1.253	3.474	0.839
0.92	7.358 (-3)	1.062 (-4)	3.374	1.336	2.949	1.189	3.252	0.765
0.94	4.022 (-3)	5.755 (-5)	3.287	1.281	2.726	1.132	3.035	0.700
0.96	2.201 (-3)	3.128 (-5)	3.206	1.231	2.509	1.082	2.824	0.640
0.98	1.206 (-3)	1.705 (-5)	3.129	1.187	2.296	1.036	2.618	0.585
1.00	6.624 (-4)	9.311 (-6)	3.056	1.146	2.087	0.995	2.415	0.535
1.02	3.645 (-4)	5.097 (-6)	2.987	1.109	1.882	0.957	2.217	0.488
1.04	2.010 (-4)	2.797 (-6)	2.921	1.076	1.681	0.922	2.022	0.444
1.06	1.111 (-4)	1.538 (-6)	2.858	1.044	1.483	0.889	1.831	0.403
1.08	6.150 (-5)	8.476 (-7)	2.798	1.015	1.289	0.859	1.643	0.364
1.10	3.411 (-5)	4.680 (-7)	2.740	0.988	1.097	0.831	1.458	0.326
1.12	1.896 (-5)	2.589 (-7)	2.685	0.962	0.908	0.805	1.275	0.291
1.14	1.055 (-5)	1.435 (-7)	2.633	0.938	0.722	0.780	1.095	0.257
1.16	5.886 (-6)	7.965 (-8)	2.582	0.916	0.538	0.757	0.918	0.225
1.18	3.288 (-6)	4.429 (-8)	2.534	0.894	0.356	0.735	0.742	0.194
1.20	1.840 (-6)	2.467 (-8)	2.488	0.874	0.176	0.714	0.569	0.164

TABLE 3 (c). THE SCATTERING MATRIX OF PERTURBATIONS APPROPRIATE TO $l = 6$
FOR THE REISSNER–NORDSTRÖM BLACK HOLE WITH CHARGE $Q_* = 0.7M$

$M\sigma$	R_1	R_2	δ_2^t	A_{12}^t	$\delta_2^{r,+}$	$A_{12}^{r,+}$	$\delta_2^{r,-}$	$A_{12}^{r,-}$
0.06	1.000	1.000	5.666	0.047	3.698	0.031	3.700	0.027
0.08	1.000	1.000	5.932	0.063	3.791	0.042	3.794	0.037
0.10	1.000	1.000	6.183	0.079	3.863	0.052	3.867	0.046
0.12	1.000	1.000	0.135	0.095	3.915	0.063	3.920	0.056
0.14	1.000	1.000	0.358	0.111	3.952	0.074	3.958	0.066
0.16	1.000	1.000	0.568	0.127	3.977	0.086	3.983	0.076
0.18	1.000	1.000	0.766	0.144	3.989	0.097	3.996	0.086
0.20	1.000	1.000	0.952	0.160	3.991	0.109	3.999	0.097
0.22	1.000	1.000	1.128	0.177	3.984	0.121	3.992	0.107
0.24	1.000	1.000	1.294	0.194	3.967	0.133	3.976	0.118
0.26	1.000	1.000	1.450	0.211	3.942	0.145	3.952	0.129
0.28	1.000	1.000	1.596	0.228	3.909	0.157	3.919	0.140
0.30	1.000	1.000	1.733	0.245	3.868	0.170	3.880	0.152
0.32	1.000	1.000	1.861	0.263	3.821	0.183	3.833	0.163
0.34	1.000	1.000	1.981	0.280	3.766	0.196	3.779	0.175
0.36	1.000	1.000	2.093	0.298	3.705	0.209	3.718	0.187
0.38	1.000	1.000	2.197	0.316	3.637	0.223	3.651	0.200
0.40	1.000	1.000	2.294	0.334	3.563	0.237	3.578	0.212
0.42	1.000	1.000	2.383	0.353	3.483	0.251	3.499	0.225
0.44	1.000	1.000	2.464	0.372	3.397	0.265	3.414	0.238
0.46	1.000	1.000	2.539	0.391	3.305	0.280	3.323	0.252
0.48	1.000	1.000	2.607	0.410	3.208	0.295	3.226	0.266
0.50	1.000	1.000	2.668	0.430	3.105	0.310	3.123	0.280
0.52	1.000	1.000	2.723	0.449	2.996	0.326	3.015	0.294
0.54	1.000	1.000	2.771	0.470	2.882	0.342	2.902	0.309
0.56	1.000	1.000	2.813	0.490	2.762	0.359	2.783	0.324
0.58	1.000	1.000	2.848	0.511	2.637	0.375	2.659	0.340
0.60	1.000	1.000	2.877	0.532	2.507	0.393	2.529	0.356
0.62	1.000	1.000	2.900	0.554	2.371	0.410	2.394	0.372
0.64	1.000	1.000	2.917	0.576	2.230	0.429	2.254	0.389
0.66	1.000	1.000	2.927	0.599	2.083	0.447	2.108	0.407
0.68	1.000	1.000	2.932	0.622	1.931	0.466	1.957	0.425
0.70	1.000	1.000	2.930	0.646	1.774	0.486	1.800	0.443
0.72	1.000	1.000	2.922	0.670	1.611	0.506	1.638	0.462
0.74	1.000	1.000	2.908	0.695	1.442	0.527	1.470	0.482
0.76	1.000	1.000	2.887	0.720	1.268	0.549	1.297	0.502
0.78	1.000	1.000	2.860	0.746	1.088	0.571	1.118	0.524
0.80	1.000	1.000	2.827	0.773	0.903	0.595	0.933	0.545
0.82	1.000	1.000	2.787	0.801	0.712	0.618	0.743	0.568
0.84	1.000	1.000	2.741	0.829	0.514	0.643	0.546	0.592
0.86	1.000	1.000	2.688	0.859	0.311	0.669	0.343	0.616
0.88	1.000	1.000	2.628	0.889	0.101	0.696	0.134	0.642
0.90	1.000	1.000	2.561	0.921	6.167	0.724	6.202	0.669
0.92	1.000	1.000	2.486	0.954	5.944	0.753	5.979	0.697

TABLE 3 (c) (*continued*)

$M\sigma$	\mathbb{R}_1	\mathbb{R}_2	δ_2^t	A_{12}^t	$\delta_2^{r,+}$	$A_{12}^{r,+}$	$\delta_2^{r,-}$	$A_{12}^{r,-}$
0.94	1.000	1.000	2.405	0.988	5.714	0.784	5.750	0.726
0.96	1.000	1.000	2.315	1.024	5.477	0.816	5.513	0.757
0.98	1.000	1.000	2.218	1.061	5.232	0.850	5.269	0.790
1.00	1.000	1.000	2.111	1.101	4.979	0.886	5.017	0.825
1.02	1.000	9.999 (-1)	1.997	1.142	4.717	0.924	4.756	0.862
1.04	1.000	9.998 (-1)	1.872	1.187	4.447	0.965	4.486	0.901
1.06	1.000	9.996 (-1)	1.738	1.234	4.167	1.009	4.207	0.944
1.08	1.000	9.993 (-1)	1.592	1.284	3.876	1.056	3.917	0.989
1.10	1.000	9.985 (-1)	1.435	1.338	3.574	1.107	3.615	1.039
1.12	9.999 (-1)	9.971 (-1)	1.265	1.398	3.259	1.163	3.301	1.094
1.14	9.999 (-1)	9.943 (-1)	1.080	1.463	2.930	1.225	2.973	1.155
1.16	9.997 (-1)	9.888 (-1)	0.878	1.536	2.584	1.295	2.628	1.224
1.18	9.995 (-1)	9.783 (-1)	0.656	1.619	2.219	1.374	2.264	1.302
1.20	9.990 (-1)	9.586 (-1)	0.412	1.714	1.832	1.466	1.877	1.392
1.22	9.980 (-1)	9.225 (-1)	0.141	1.824	1.418	1.572	1.464	1.497
1.24	9.962 (-1)	8.600 (-1)	6.124	1.950	0.975	1.695	1.022	1.619
1.26	9.928 (-1)	7.606 (-1)	5.793	2.093	0.502	1.835	0.550	1.757
1.28	9.862 (-1)	6.224 (-1)	5.436	2.244	0.004	1.983	0.052	1.904
1.30	9.738 (-1)	4.617 (-1)	5.066	2.389	5.776	2.125	5.825	2.045
1.32	9.512 (-1)	3.091 (-1)	4.701	2.507	5.269	2.239	5.319	2.159
1.34	9.108 (-1)	1.896 (-1)	4.355	2.579	4.783	2.308	4.833	2.226
1.36	8.430 (-1)	1.093 (-1)	4.038	2.594	4.325	2.320	4.376	2.237
1.38	7.388 (-1)	6.056 (-2)	3.750	2.552	3.896	2.275	3.948	2.190
1.40	5.991 (-1)	3.285 (-2)	3.488	2.459	3.494	2.179	3.547	2.094
1.42	4.417 (-1)	1.762 (-2)	3.249	2.334	3.116	2.051	3.169	1.964
1.44	2.957 (-1)	9.401 (-3)	3.029	2.196	2.756	1.910	2.811	1.822
1.46	1.825 (-1)	5.008 (-3)	2.825	2.062	2.413	1.773	2.468	1.683
1.48	1.063 (-1)	2.668 (-3)	2.635	1.941	2.084	1.649	2.140	1.558
1.50	5.972 (-2)	1.422 (-3)	2.456	1.837	1.766	1.541	1.823	1.449
1.52	3.286 (-2)	7.595 (-4)	2.287	1.747	1.459	1.449	1.517	1.355
1.54	1.789 (-2)	4.061 (-4)	2.127	1.670	1.161	1.369	1.219	1.274
1.56	9.685 (-3)	2.176 (-4)	1.975	1.603	0.871	1.299	0.930	1.203
1.58	5.234 (-3)	1.168 (-4)	1.830	1.545	0.588	1.237	0.648	1.141
1.60	2.827 (-3)	6.276 (-5)	1.692	1.493	0.313	1.182	0.373	1.084
1.62	1.528 (-3)	3.379 (-5)	1.560	1.446	0.043	1.133	0.104	1.033
1.64	8.270 (-4)	1.823 (-5)	1.433	1.403	6.062	1.087	6.124	0.987
1.66	4.481 (-4)	9.846 (-6)	1.311	1.365	5.803	1.046	5.866	0.944
1.68	2.431 (-4)	5.327 (-6)	1.193	1.329	5.549	1.007	5.612	0.904
1.70	1.321 (-4)	2.887 (-6)	1.080	1.296	5.299	0.971	5.364	0.867
1.72	7.188 (-5)	1.567 (-6)	0.971	1.265	5.054	0.938	5.119	0.832
1.74	3.917 (-5)	8.516 (-7)	0.866	1.236	4.813	0.906	4.878	0.799
1.76	2.137 (-5)	4.635 (-7)	0.764	1.209	4.575	0.876	4.642	0.768
1.78	1.168 (-5)	2.526 (-7)	0.666	1.184	4.341	0.848	4.408	0.738
1.80	6.391 (-6)	1.379 (-7)	0.570	1.159	4.110	0.821	4.178	0.710

PERTURBATIONS OF REISSNER–NORDSTRÖM BLACK HOLE 521

TABLE 4 (*a*). THE SCATTERING MATRIX OF PERTURBATIONS APPROPRIATE TO $l = 2$
FOR THE REISSNER–NORDSTRÖM BLACK HOLE WITH CHARGE $Q_* = 0.99M$

$M\sigma$	\mathbb{R}_1	\mathbb{R}_2	δ_2^t	A_{12}^t	$\delta_2^{r,+}$	$A_{12}^{r,+}$	$\delta_2^{r,-}$	$A_{12}^{r,-}$
0.02	1.000	1.000	5.082	0.167	3.322	0.067	3.348	0.034
0.04	1.000	1.000	5.379	0.335	3.383	0.136	3.437	0.070
0.06	1.000	1.000	5.631	0.503	3.399	0.207	3.479	0.108
0.08	1.000	1.000	5.840	0.670	3.383	0.281	3.489	0.149
0.10	1.000	1.000	6.009	0.837	3.341	0.357	3.473	0.192
0.12	1.000	1.000	6.141	1.002	3.276	0.436	3.435	0.237
0.14	1.000	1.000	6.241	1.167	3.192	0.518	3.377	0.286
0.16	1.000	1.000	0.028	1.331	3.089	0.603	3.301	0.339
0.18	1.000	1.000	0.072	1.494	2.969	0.692	3.207	0.395
0.20	1.000	1.000	0.090	1.658	2.831	0.786	3.095	0.456
0.22	1.000	9.999 (-1)	0.084	1.822	2.677	0.885	2.967	0.523
0.24	1.000	9.997 (-1)	0.055	1.989	2.504	0.990	2.820	0.595
0.26	1.000	9.992 (-1)	0.003	2.159	2.314	1.102	2.656	0.675
0.28	1.000	9.980 (-1)	6.211	2.333	2.104	1.224	2.471	0.764
0.30	1.000	9.952 (-1)	6.110	2.515	1.872	1.356	2.265	0.864
0.32	1.000	9.887 (-1)	5.983	2.707	1.616	1.502	2.035	0.978
0.34	1.000	9.741 (-1)	5.824	2.914	1.332	1.666	1.776	1.110
0.36	1.000	9.433 (-1)	5.630	3.141	1.014	1.853	1.483	1.265
0.38	1.000	8.823 (-1)	5.395	3.392	0.658	2.067	1.153	1.448
0.40	1.000	7.747 (-1)	5.119	3.670	0.262	2.311	0.782	1.660
0.42	1.000	6.157 (-1)	4.809	3.967	6.117	2.576	0.378	1.895
0.44	9.999 (-1)	4.310 (-1)	4.484	4.263	5.676	2.843	6.244	2.130
0.46	9.999 (-1)	2.663 (-1)	4.172	4.531	5.248	3.084	5.840	2.341
0.48	9.997 (-1)	1.497 (-1)	3.890	4.753	4.851	3.281	5.468	2.507
0.50	9.993 (-1)	7.949 (-2)	3.645	4.921	4.493	3.427	5.134	2.622
0.52	9.985 (-1)	4.104 (-2)	3.434	5.038	4.169	3.522	4.834	2.687
0.54	9.967 (-1)	2.096 (-2)	3.252	5.107	3.876	3.572	4.564	2.707
0.56	9.929 (-1)	1.069 (-2)	3.093	5.131	3.605	3.579	4.317	2.684
0.58	9.849 (-1)	5.466 (-3)	2.952	5.114	3.354	3.546	4.090	2.621
0.60	9.686 (-1)	2.810 (-3)	2.826	5.055	3.119	3.472	3.877	2.517
0.62	9.365 (-1)	1.453 (-3)	2.713	4.952	2.896	3.355	3.677	2.371
0.64	8.764 (-1)	7.555 (-4)	2.610	4.802	2.684	3.193	3.488	2.180
0.66	7.746 (-1)	3.952 (-4)	2.515	4.606	2.482	2.986	3.308	1.944
0.68	6.264 (-1)	2.079 (-4)	2.428	4.371	2.287	2.740	3.135	1.670
0.70	4.517 (-1)	1.100 (-4)	2.347	4.113	2.099	2.473	2.969	1.374
0.72	2.894 (-1)	5.845 (-5)	2.272	3.856	1.917	2.208	2.809	1.081
0.74	1.684 (-1)	3.122 (-5)	2.202	3.618	1.741	1.963	2.655	0.808
0.76	9.198 (-2)	1.675 (-5)	2.137	3.409	1.570	1.747	2.505	0.565
0.78	4.847 (-2)	9.026 (-6)	2.076	3.229	1.403	1.561	2.359	0.351
0.80	2.511 (-2)	4.883 (-6)	2.018	3.073	1.240	1.400	2.217	0.162
0.82	1.291 (-2)	2.652 (-6)	1.964	2.937	1.081	1.259	2.078	6.278
0.84	6.634 (-3)	1.446 (-6)	1.912	2.818	0.925	1.136	1.942	6.127
0.86	3.413 (-3)	7.909 (-7)	1.864	2.711	0.772	1.025	1.810	5.990
0.88	1.760 (-3)	4.341 (-7)	1.818	2.614	0.622	0.926	1.680	5.865
0.90	9.111 (-4)	2.390 (-7)	1.774	2.526	0.475	0.835	1.552	5.748
0.92	4.732 (-4)	1.320 (-7)	1.732	2.446	0.330	0.753	1.426	5.640
0.94	2.467 (-4)	7.307 (-8)	1.693	2.371	0.187	0.677	1.303	5.538
0.96	1.290 (-4)	4.057 (-8)	1.655	2.302	0.046	0.607	1.181	5.443
0.98	6.773 (-5)	2.259 (-8)	1.619	2.238	6.190	0.542	1.061	5.352
1.00	3.567 (-5)	1.261 (-8)	1.585	2.178	6.054	0.481	0.943	5.267
1.02	1.884 (-5)	7.052 (-9)	1.552	2.121	5.918	0.424	0.826	5.186
1.04	9.987 (-6)	3.954 (-9)	1.520	2.068	5.785	0.372	0.710	5.108
1.06	5.309 (-6)	2.222 (-9)	1.490	2.018	5.653	0.322	0.596	5.034
1.08	2.830 (-6)	1.251 (-9)	1.461	1.971	5.522	0.275	0.483	4.963
1.10	1.513 (-6)	7.058 (-10)	1.433	1.926	5.393	0.231	0.371	4.896

TABLE 4(b). THE SCATTERING MATRIX OF PERTURBATIONS APPROPRIATE TO $l = 3$
FOR THE REISSNER-NORDSTRÖM BLACK HOLE WITH CHARGE $Q_* = 0.99M$

$M\sigma$	\mathbb{R}_1	\mathbb{R}_2	δ_2^t	Δ_{12}^t	$\delta_2^{r,+}$	$\Delta_{12}^{r,+}$	$\delta_2^{r,-}$	$\Delta_{12}^{r,-}$
0.04	1.000	1.000	0.939	0.220	0.419	0.066	0.432	0.047
0.06	1.000	1.000	1.299	0.330	0.469	0.100	0.489	0.073
0.08	1.000	1.000	1.626	0.440	0.508	0.136	0.535	0.099
0.10	1.000	1.000	1.915	0.550	0.531	0.172	0.564	0.126
0.12	1.000	1.000	2.170	0.659	0.536	0.209	0.576	0.154
0.14	1.000	1.000	2.393	0.768	0.526	0.248	0.573	0.183
0.16	1.000	1.000	2.586	0.876	0.502	0.287	0.555	0.213
0.18	1.000	1.000	2.754	0.983	0.464	0.328	0.524	0.244
0.20	1.000	1.000	2.898	1.090	0.414	0.370	0.480	0.278
0.22	1.000	1.000	3.020	1.196	0.352	0.413	0.425	0.311
0.24	1.000	1.000	3.123	1.302	0.279	0.458	0.358	0.347
0.26	1.000	1.000	3.207	1.407	0.194	0.504	0.281	0.384
0.28	1.000	1.000	3.274	1.511	0.100	0.552	0.192	0.422
0.30	1.000	1.000	3.325	1.616	0.277	0.602	0.094	0.463
0.32	1.000	1.000	3.360	1.720	0.162	0.654	0.268	0.506
0.34	1.000	1.000	3.380	1.824	0.036	0.708	0.148	0.551
0.36	1.000	1.000	3.385	1.929	0.899	0.765	0.018	0.598
0.38	1.000	1.000	3.377	2.035	0.752	0.824	0.878	0.648
0.40	1.000	1.000	3.354	2.141	0.595	0.886	0.727	0.701
0.42	1.000	1.000	3.318	2.250	0.427	0.952	0.566	0.758
0.44	1.000	1.000	3.267	2.360	0.247	1.021	0.393	0.818
0.46	1.000	9.999 (-1)	3.203	2.472	0.056	1.095	0.208	0.882
0.48	1.000	9.998 (-1)	3.123	2.588	0.852	1.174	0.011	0.952
0.50	1.000	9.996 (-1)	3.029	2.708	0.635	1.258	0.800	1.027
0.52	1.000	9.990 (-1)	2.918	2.833	0.403	1.349	0.575	1.109
0.54	1.000	9.979 (-1)	2.790	2.965	0.156	1.448	0.334	1.199
0.56	1.000	9.953 (-1)	2.642	3.105	0.891	1.557	0.076	1.299
0.58	1.000	9.897 (-1)	2.472	3.256	0.605	1.679	0.797	1.411
0.60	1.000	9.780 (-1)	2.278	3.422	0.296	1.816	0.494	1.539
0.62	1.000	9.540 (-1)	2.053	3.606	0.958	1.973	0.162	1.687
0.64	1.000	9.072 (-1)	1.795	3.814	0.586	2.155	0.798	1.860
0.66	1.000	8.230 (-1)	1.498	4.049	0.178	2.365	0.396	2.060
0.68	1.000	6.902 (-1)	1.165	4.307	0.735	2.600	0.959	2.286
0.70	9.999 (-1)	5.184 (-1)	0.809	4.577	1.269	2.847	0.500	2.524
0.72	9.998 (-1)	3.438 (-1)	0.452	4.836	0.803	3.084	0.041	2.752
0.74	9.996 (-1)	2.043 (-1)	0.116	5.060	0.359	3.288	0.603	2.946
0.76	9.991 (-1)	1.125 (-1)	0.096	5.237	0.232	3.444	0.199	3.094
0.78	9.982 (-1)	5.920 (-2)	0.829	5.363	0.858	3.551	0.115	3.192
0.80	9.961 (-1)	3.048 (-2)	0.593	5.440	0.515	3.611	0.779	3.242
0.82	9.919 (-1)	1.555 (-2)	0.383	5.472	0.200	3.625	0.470	3.248
0.84	9.832 (-1)	7.914 (-3)	0.194	5.461	0.906	3.597	0.183	3.210
0.86	9.658 (-1)	4.034 (-3)	0.023	5.406	0.630	3.527	0.913	3.131
0.88	9.318 (-1)	2.062 (-3)	0.866	5.307	0.370	3.412	0.659	3.007
0.90	8.694 (-1)	1.058 (-3)	0.722	5.160	0.121	3.251	0.417	2.837
0.92	7.652 (-1)	5.452 (-4)	0.488	4.967	0.884	3.044	0.187	2.621
0.94	6.158 (-1)	2.820 (-4)	0.463	4.735	0.656	2.799	0.965	2.366
0.96	4.421 (-1)	1.465 (-4)	0.346	4.481	0.436	2.531	0.752	2.090
0.98	2.824 (-1)	7.634 (-5)	0.235	4.227	0.224	2.266	0.546	1.815
1.00	1.641 (-1)	3.994 (-5)	0.132	3.993	0.019	2.019	0.347	1.560
1.02	8.954 (-2)	2.097 (-5)	0.034	3.786	0.819	1.801	0.154	1.333
1.04	4.714 (-2)	1.105 (-5)	0.941	3.607	0.625	1.611	0.966	1.134
1.06	2.437 (-2)	5.842 (-6)	0.853	3.451	0.436	1.446	0.783	0.959
1.08	1.251 (-2)	3.098 (-6)	0.769	3.315	0.251	1.300	0.605	0.804
1.10	6.403 (-3)	1.648 (-6)	0.689	3.195	0.071	1.170	0.431	0.665
1.12	3.280 (-3)	8.791 (-7)	0.612	3.087	0.894	0.053	2.261	0.539
1.14	1.683 (-3)	4.703 (-7)	0.539	2.989	0.721	0.946	0.205	0.423
1.16	8.660 (-4)	2.523 (-7)	0.470	2.899	0.552	0.849	1.932	0.317
1.18	4.469 (-4)	1.357 (-7)	0.303	2.817	0.385	0.758	1.772	0.217
1.20	2.312 (-4)	7.316 (-8)	0.339	2.740	0.222	0.674	1.615	0.124
1.22	1.200 (-4)	3.954 (-8)	0.277	2.669	0.061	0.596	1.460	0.037
1.24	6.246 (-5)	2.142 (-8)	0.218	2.603	0.903	0.523	1.309	0.238
1.26	3.260 (-5)	1.163 (-8)	0.161	2.540	0.747	0.454	1.159	0.160
1.28	1.706 (-5)	6.329 (-9)	0.106	2.482	0.594	0.389	1.012	0.086
1.30	8.952 (-6)	3.451 (-9)	0.053	2.426	0.443	0.327	0.867	0.015

PERTURBATIONS OF REISSNER-NORDSTRÖM BLACK HOLE 523

TABLE 4 (*c*). THE SCATTERING MATRIX OF PERTURBATIONS APPROPRIATE TO $l = 6$
FOR THE REISSNER-NORDSTRÖM BLACK HOLE WITH CHARGE $Q_* = 0.99M$

$M\sigma$	R_1	R_2	δ_2^t	A_{12}^t	δ_2^{r+}	A_{12}^{r+}	δ_2^{r-}	A_{12}^{r-}
0.06	1.000	1.000	0.248	0.169	3.791	0.041	3.793	0.038
0.08	1.000	1.000	0.759	0.226	3.915	0.056	3.918	0.051
0.10	1.000	1.000	1.230	0.282	4.019	0.070	4.022	0.064
0.12	1.000	1.000	1.665	0.339	4.103	0.085	4.107	0.077
0.14	1.000	1.000	2.066	0.395	4.172	0.099	4.177	0.091
0.16	1.000	1.000	2.438	0.451	4.228	0.114	4.234	0.105
0.18	1.000	1.000	2.784	0.508	4.273	0.130	4.279	0.119
0.20	1.000	1.000	3.105	0.564	4.307	0.145	4.314	0.133
0.22	1.000	1.000	3.405	0.619	4.332	0.161	4.340	0.147
0.24	1.000	1.000	3.685	0.675	4.348	0.177	4.357	0.162
0.26	1.000	1.000	3.947	0.731	4.355	0.193	4.365	0.177
0.28	1.000	1.000	4.192	0.786	4.355	0.210	4.366	0.193
0.30	1.000	1.000	4.421	0.841	4.348	0.227	4.359	0.208
0.32	1.000	1.000	4.635	0.896	4.334	0.244	4.346	0.224
0.34	1.000	1.000	4.835	0.951	4.312	0.261	4.325	0.241
0.36	1.000	1.000	5.022	1.005	4.285	0.279	4.299	0.257
0.38	1.000	1.000	5.196	1.059	4.251	0.297	4.266	0.274
0.40	1.000	1.000	5.359	1.113	4.212	0.316	4.227	0.291
0.42	1.000	1.000	5.511	1.167	4.166	0.334	4.182	0.309
0.44	1.000	1.000	5.651	1.221	4.115	0.354	4.132	0.327
0.46	1.000	1.000	5.782	1.274	4.059	0.373	4.076	0.345
0.48	1.000	1.000	5.903	1.327	3.997	0.393	4.015	0.364
0.50	1.000	1.000	6.014	1.380	3.929	0.413	3.948	0.383
0.52	1.000	1.000	6.116	1.433	3.857	0.434	3.877	0.402
0.54	1.000	1.000	6.210	1.486	3.779	0.455	3.800	0.422
0.56	1.000	1.000	0.011	1.538	3.697	0.477	3.718	0.442
0.58	1.000	1.000	0.088	1.590	3.609	0.499	3.631	0.463
0.60	1.000	1.000	0.157	1.643	3.516	0.521	3.539	0.485
0.62	1.000	1.000	0.217	1.695	3.419	0.544	3.442	0.506
0.64	1.000	1.000	0.271	1.747	3.316	0.568	3.340	0.529
0.66	1.000	1.000	0.316	1.799	3.209	0.592	3.234	0.552
0.68	1.000	1.000	0.355	1.851	3.097	0.617	3.122	0.575
0.70	1.000	1.000	0.386	1.904	2.980	0.642	3.006	0.600
0.72	1.000	1.000	0.410	1.956	2.858	0.668	2.885	0.624
0.74	1.000	1.000	0.427	2.008	2.731	0.695	2.759	0.650
0.76	1.000	1.000	0.438	2.061	2.599	0.723	2.628	0.676
0.78	1.000	1.000	0.441	2.114	2.463	0.751	2.492	0.703
0.80	1.000	1.000	0.438	2.167	2.321	0.780	2.352	0.731
0.82	1.000	1.000	0.428	2.220	2.175	0.810	2.206	0.759
0.84	1.000	1.000	0.412	2.274	2.023	0.840	2.055	0.789
0.86	1.000	1.000	0.389	2.328	1.867	0.872	1.899	0.819
0.88	1.000	1.000	0.359	2.383	1.705	0.904	1.738	0.850
0.90	1.000	1.000	0.323	2.438	1.538	0.938	1.572	0.883
0.92	1.000	1.000	0.280	2.494	1.366	0.973	1.400	0.916
0.94	1.000	1.000	0.230	2.551	1.188	1.009	1.223	0.951
0.96	1.000	1.000	0.174	2.609	1.004	1.046	1.041	0.987
0.98	1.000	1.000	0.111	2.667	0.816	1.085	0.853	1.025

TABLE 4(c) (*continued*)

$M\sigma$	\mathbb{R}_1	\mathbb{R}_2	δ_2^t	A_{12}^t	$\delta_2^{r,+}$	$A_{12}^{r,+}$	$\delta_2^{r,-}$	$A_{12}^{r,-}$
1.00	1.000	1.000	0.040	2.726	0.621	1.125	0.658	1.063
1.02	1.000	1.000	6.246	2.787	0.420	1.166	0.458	1.104
1.04	1.000	1.000	6.162	2.849	0.213	1.210	0.252	1.146
1.06	1.000	1.000	6.070	2.912	6.283	1.255	0.040	1.190
1.08	1.000	1.000	5.971	2.977	6.063	1.302	6.104	1.236
1.10	1.000	1.000	5.864	3.044	5.836	1.351	5.878	1.284
1.12	1.000	1.000	5.749	3.113	5.602	1.403	5.645	1.335
1.14	1.000	1.000	5.626	3.184	5.361	1.458	5.404	1.388
1.16	1.000	1.000	5.494	3.258	5.112	1.515	5.156	1.444
1.18	1.000	1.000	5.353	3.334	4.854	1.576	4.899	1.503
1.20	1.000	9.999 (-1)	5.202	3.414	4.588	1.640	4.633	1.566
1.22	1.000	9.999 (-1)	5.042	3.498	4.312	1.708	4.358	1.634
1.24	1.000	9.997 (-1)	4.870	3.586	4.026	1.782	4.073	1.706
1.26	1.000	9.994 (-1)	4.687	3.680	3.729	1.860	3.776	1.783
1.28	1.000	9.988 (-1)	4.490	3.779	3.419	1.946	3.467	1.867
1.30	1.000	9.976 (-1)	4.280	3.886	3.096	2.039	3.145	1.959
1.32	1.000	9.949 (-1)	4.053	4.003	2.757	2.141	2.806	2.060
1.34	1.000	9.896 (-1)	3.807	4.130	2.399	2.255	2.450	2.173
1.36	1.000	9.786 (-1)	3.539	4.272	2.021	2.384	2.072	2.300
1.38	1.000	9.569 (-1)	3.245	4.432	1.616	2.531	1.668	2.446
1.40	1.000	9.154 (-1)	2.920	4.615	1.181	2.701	1.234	2.615
1.42	1.000	8.411 (-1)	2.561	4.824	0.712	2.897	0.766	2.810
1.44	9.999 (-1)	7.220 (-1)	2.166	5.058	0.209	3.119	0.263	3.031
1.46	9.999 (-1)	5.611 (-1)	1.746	5.308	5.964	3.357	6.019	3.268
1.48	9.997 (-1)	3.870 (-1)	1.319	5.555	5.428	3.592	5.484	3.502
1.50	9.995 (-1)	2.383 (-1)	0.907	5.775	4.908	3.801	4.965	3.709
1.52	9.989 (-1)	1.346 (-1)	0.525	5.953	4.419	3.968	4.476	3.875
1.54	9.977 (-1)	7.194 (-2)	0.178	6.082	3.965	4.086	4.023	3.992
1.56	9.952 (-1)	3.731 (-2)	6.146	6.163	3.543	4.156	3.602	4.060
1.58	9.903 (-1)	1.907 (-2)	5.859	6.197	3.150	4.180	3.210	4.083
1.60	9.803 (-1)	9.681 (-3)	5.596	6.188	2.781	4.160	2.841	4.062
1.62	9.606 (-1)	4.906 (-3)	5.351	6.134	2.431	4.096	2.492	3.997
1.64	9.229 (-1)	2.487 (-3)	5.123	6.034	2.097	3.987	2.159	3.886
1.66	8.552 (-1)	1.262 (-3)	4.909	5.887	1.778	3.830	1.840	3.728
1.68	7.448 (-1)	6.419 (-4)	4.706	5.694	1.471	3.627	1.534	3.524
1.70	5.913 (-1)	3.272 (-4)	4.514	5.462	1.174	3.385	1.238	3.281
1.72	4.183 (-1)	1.671 (-4)	4.331	5.210	0.887	3.124	0.952	3.019
1.74	2.638 (-1)	8.559 (-5)	4.156	4.961	0.609	2.866	0.675	2.759
1.76	1.518 (-1)	4.392 (-5)	3.989	4.731	0.338	2.627	0.405	2.519
1.78	8.225 (-2)	2.259 (-5)	3.829	4.528	0.075	2.416	0.142	2.306
1.80	4.305 (-2)	1.165 (-5)	3.675	4.352	6.102	2.231	6.170	2.120
1.82	2.214 (-2)	6.016 (-6)	3.527	4.198	5.851	2.068	5.920	1.957
1.84	1.129 (-2)	3.115 (-6)	3.385	4.062	5.606	1.925	5.675	1.812
1.86	5.738 (-3)	1.616 (-6)	3.248	3.942	5.366	1.796	5.437	1.682
1.88	2.916 (-3)	8.399 (-7)	3.115	3.833	5.132	1.679	5.203	1.564
1.90	1.482 (-3)	4.374 (-7)	2.987	3.734	4.902	1.572	4.973	1.456

TABLE 5. THE COMPLEX FREQUENCIES ($M\sigma$) BELONGING TO THE QUASI-NORMAL MODES OF Z_1

Q_*	$l = 1$	$l = 2$	$l = 3$	$l = 4$	$l = 5$	$l = 6$
0.0	0.24828 + 0.09250i	0.45760 + 0.09500i	0.65690 + 0.09562i	0.85310 + 0.09586i	1.04791 + 0.09598i	1.24200 + 0.096051i
0.1	0.24908 + 0.09260i	0.45893 + 0.09510i	0.65876 + 0.09579i	0.85549 + 0.09595i	1.05083 + 0.09607i	1.24542 + 0.096139i
0.2	0.25150 + 0.09291i	0.46296 + 0.09537i	0.66437 + 0.09597i	0.86260 + 0.09621i	1.05938 + 0.09633i	1.25537 + 0.096389i
0.3	0.25569 + 0.09343i	0.46987 + 0.09583i	0.67379 + 0.09640i	0.87437 + 0.09662i	1.07336 + 0.09672i	1.27143 + 0.096775i
0.4	0.26194 + 0.09416i	0.47993 + 0.09644i	0.68728 + 0.09697i	0.89100 + 0.09716i	1.09291 + 0.09724i	1.29378 + 0.097270i
0.5	0.27070 + 0.09509i	0.49368 + 0.09719i	0.70540 + 0.09765i	0.91310 + 0.09779i	1.11879 + 0.09783i	1.32329 + 0.097840i
0.6	0.28276 + 0.09619i	0.51201 + 0.09802i	0.72919 + 0.09837i	0.94192 + 0.09845i	1.15243 + 0.09845i	1.36164 + 0.098420i
0.7	0.29948 + 0.09737i	0.53651 + 0.09877i	0.76050 + 0.09898i	0.97966 + 0.09898i	1.19640 + 0.09893i	1.41176 + 0.098874i
0.8	0.32349 + 0.09827i	0.57013 + 0.09907i	0.80284 + 0.09911i	1.03039 + 0.09903i	1.25541 + 0.09894i	1.47899 + 0.098847i
0.85	0.33984 + 0.09827i	0.59212 + 0.09872i	0.83019 + 0.09869i	1.06301 + 0.09858i	1.29327 + 0.09847i	1.52206 + 0.098374i
0.9	0.36082 + 0.09744i	0.61939 + 0.09758i	0.86375 + 0.09752i	1.10286 + 0.09742i	1.33940 + 0.09731i	1.57449 + 0.097214i
0.925	0.37384 + 0.09636i	0.63581 + 0.09644i	0.88376 + 0.09642i	1.12650 + 0.09633i	1.36671 + 0.09625i	1.60548 + 0.096168i
0.95	0.38927 + 0.09442i	0.65476 + 0.09460i	0.90668 + 0.09469i	1.1535 + 0.09467i	1.39784 + 0.09463i	1.64076 + 0.094582i
0.99	0.42139 + 0.08710i	0.69275 + 0.08864i	0.95206 + 0.08932	1.20665 + 0.08963i	1.45889 + 0.08979i	1.70980 + 0.089885i
0.999	0.43031 + 0.08388i	0.70310 + 0.08627i	0.96434i + 0.08726i	1.22097 + 0.08773i	1.47529 + 0.08799i	1.72831 + 0.088147i

TABLE 6. THE COMPLEX FREQUENCIES ($M\sigma$) BELONGING TO THE QUASI-NORMAL MODES OF Z_2

Q_*	$l = 1$	$l = 2$	$l = 3$	$l = 4$	$l = 5$	$l = 6$
0.0	0.11252 + 0.10040i	0.37367 + 0.08896i	0.59944 + 0.09270i	0.80918 + 0.09416i	1.01229 + 0.094870i	1.21201 + 0.095266i
0.1	0.11269 + 0.10045i	0.37393 + 0.08899i	0.59982 + 0.09272i	0.80967 + 0.09418i	1.01291 + 0.094890i	1.21276 + 0.095285i
0.2	0.11320 + 0.10061i	0.37475 + 0.08907i	0.60103 + 0.09279i	0.81134 + 0.09425i	1.01510 + 0.094956i	1.21552 + 0.095355i
0.3	0.11407 + 0.10088i	0.37620 + 0.08921i	0.60333 + 0.09290i	0.81467 + 0.09436i	1.01860 + 0.095082i	1.22131 + 0.095690i
0.4	0.11537 + 0.10123i	0.37844 + 0.08940i	0.60705 + 0.09306i	0.82020 + 0.09453i	1.02715 + 0.095266i	1.23100 + 0.095690i
0.5	0.11716 + 0.10165i	0.38168 + 0.08961i	0.61265 + 0.09324i	0.82858 + 0.09474i	1.03853 + 0.095492i	1.24553 + 0.095936i
0.6	0.11957 + 0.10206i	0.38622 + 0.08981i	0.62066 + 0.09341i	0.84056 + 0.09493i	1.05472 + 0.095709i	1.26604 + 0.096175i
0.7	0.12279 + 0.10230i	0.39250 + 0.08990i	0.63187 + 0.09312i	0.85727 + 0.09500i	1.07716 + 0.095803i	1.29433 + 0.096290i
0.8	1.12712 + 0.10198i	0.40122 + 0.08964i	0.64755 + 0.09312i	0.88057 + 0.09467i	1.10831 + 0.095489i	1.33345 + 0.095991i
0.85	0.12979 + 0.10129i	0.40683 + 0.08920i	0.65772 + 0.09261i	0.89566 + 0.09415i	1.12847 + 0.094969i	1.35872 + 0.09547i
0.9	0.13276 + 0.09980i	0.41357 + 0.08833i	0.67002 + 0.09164i	0.91396 + 0.09314i	1.15291 + 0.093938i	1.38937 + 0.094425i
0.925	1.13422 + 0.09854i	0.41744 + 0.08763i	0.67719 + 0.09087i	0.92465 + 0.09232i	1.16721 + 0.093095i	1.40733 + 0.093564i
0.95	0.13540 + 0.09675i	0.42169 + 0.08666i	0.68519 + 0.08978i	0.93664 + 0.09117i	1.18329 + 0.091896i	1.42753 + 0.09234i
0.99	0.13463 + 0.09385i	0.42930 + 0.08427i	0.70010 + 0.08698i	0.95928 + 0.08813i	1.21381 + 0.088699i	1.46603 + 0.089025i
0.999	0.13416 + 0.09666i	0.43113 + 0.08354i	0.70387 + 0.08608i	0.96510 + 0.08712i	1.22172 + 0.087625i	1.47605 + 0.087902i